UNIVERSITA' DEGLI STUDI DI NAPOLI FEDERICO II

Dipartimento di Ingegneria Chimica, dei Materiali e della Produzione Industriale

Ph.D. IN MATERIALS AND STRUCTURES ENGINEERING

(XXVII CYCLE)

"*Tissue-engineered matrix as functional delivery system: Controlled release of bioactive pro-angiogenic peptide from degradable PCL scaffold.*"

Advisor	Tutor
Prof. Paolo Antonio Netti	Ing. Lucio Rossi
Cordinator	Candidate
Prof. Giuseppe Mensitieri	Emanuela Vilardi

2012 - 2015

Abstract

Several studies in the field of tissue engineering have led to the conclusion that the success of a graft designed to ensure the regeneration / repair of a tissue is closely related to its ability of inducing the formation of a vascular network capable of supporting the function of those cells that will make up the newly formed tissue.

In tissue engineering in fact, angiogenesis - the development of new blood vessels from existing ones - is a process of fundamental importance in many physiological processes such as normal tissue growth, being responsible of creating a vascular network capable of providing oxygen and nutrients to the neo-formed tissue.

Vessel formation is characterized by several stages such as the recruitment and differentiation of endothelial progenitor cells, and is mediated by specific soluble growth factors, such as Vascular-Endothelial Growth Factor.

Biocompatible scaffolds represent a valuable structural support, but also as a potential guide for regenerative processes. They must satisfy specific physical and mechanical properties, such as a high, interconnected porosity, mechanical strength and in addition to satisfying the obvious requests of biocompatibility, it is envisioned that next-generation scaffolds will be designed with the capability of controlling a specific bio-signals release.

This work aims to analyze the bioactive potential of a scaffold designed with a “bottom up” technique in which the construct is seen as the assembly of single units (building blocks) each with its on specific, pre-designed, function.

Followig the bottom-up paradigm, we developed an assembly procedure based on solvent sinterization of microspherical building blocks. Constructs fabricated by this technique, are multifunctional polymer scaffolds with predefined pore dimension and high interconnectivity. These constructs were loaded with interspersing PLGA drug delivery systems (DDSs) for the release of angiogenic factors or similar molecules.

Specifically, QK, the "engineered VEGF mimicking peptide" was loaded onto these DDS.

We wanted to demonstrate that QK maintains its pro-angiogenic activity in the context of an application in which PCL scaffolds, made following a bottom up approach, are loaded with DDS controlled release.

Table of Contents

Chapter 1

1. Introduction

1.1. Vascular tissue development

Vascularization is a key factor in tissue engineering (TE) supporting the successful integration of grafts inside the host body. The vascular system provides a number of critical functions, including the delivery of oxygen and nutrients to all parts of the body, transport of metabolic waste products, and delivery of circulating soluble factors, and stem and progenitor cells [1]. Development of a stable and functional vascular system depends on the balance of the angiogenic signals and other signals that promote the regression of vessel themselves. Indeed, in pathological conditions, the angiogenic process is very abnormal due to an alteration of this homeostasis.

Vascularization is initiated during embryonic development, and the development of the cardiovascular system precedes the developments of all other organs in the embryo due to its central importance [2]. Vascularization continues during postnatal growth and in the adult during the menstrual cycle, inflammation and wound healing. It is generally believed that neovascularization includes three processes, namely vasculogenesis, angiogenesis, arteriogenesis [3]. In the embryo, vasculogenesis is the *de novo* vessel network formation from angioblasts or endothelial progenitor cells that migrate, proliferate and differentiate to form endothelial cells, and subsequently organize into cord-like structures as the primary plexus [4].

Angiogenesis refers to the process of blood vessel sprouting from preexisting capillaries, and includes subsequent remodeling

processes such as pruning, vessel enlargement, and intussusceptions (vessel splitting) to form stable vessel networks [5]. This process unfolds in four phases characterized by different genetic programs that include the activation and migration of existing mature endothelial cells, degradation and remodeling of extra cellular matrix (ECM), endothelial cell proliferation and the formation of new blood vessels. These phases are summarized hereunder:

- ✓ Recruitment and differentiation of endothelial progenitor cells by soluble factors (VEGF, P1GF, Ang1, cytokine)
- ✓ Quiescent of endothelial cells and interaction with the major component of the ECM
- ✓ Activation of ECs, proliferation, migration through the release of metalloproteinase (MMPs) and plasmin
- ✓ Differentiation and morphogenesis of endothelial cells. Recruitment of smooth muscle cells (SMC) by soluble factors
- ✓ Stabilization of vessels

Under the action of angiogenic factors, endothelial cells produce proteolytic enzymes (MMPs) that degrade the basement membrane of pre-existing capillary and express specification integrins for migration. Endothelial cells migrate towards the source of the angiogenic factor where they will form a new vessel.

Finally, arteriogenesis mainly denotes the enlargement of arterial vessels to adjust for lost flow in other vessels [6] and these terms are also used at times to include the process of remodeling of existing capillaries to form arterioles [7].

All vascularization processes involve a series of interactions among cytokines, growth factors, various types of cells and enzymes. Numerous growth factors involved in vasculogenesis have been identified and characterized, including vascular endothelial growth factor (VEGF) Fibroblast growth factor (FGF), Placenta growth factor (PIGF), Hepatocyte growth factor (HGF), Platelet-derived growth factor (PDGF), Angiopoietin-1 and Angiopoietin-2, insulin-like growth factor (IGF), granulocyte macrophage colony-stimulating factor (GM-CSF), and monocyte chemo-attractant protein-1 (MCP-1). The mechanism that regulates this interaction is altered either by a reduction of inhibitory factors - as it happens in most common heart disease - or by excessive production and release of pro-angiogenic factors, typical of tumor-associated angiogenesis.

1.2. 3D Scaffold for bone regeneration

In order to regenerate a natural tissue the use of a three-dimensional structure inducing tissue re-growth with specific stimuli seems mandatory. Recent studies show that isolated cells are hardly capable of organizing them spontaneously to form complex tissue in absence of three-dimensional structures able to guide and stimulate their activity [8]. The three-dimensional tissue regeneration requires, therefore, a support (scaffold) that emulates the extracellular matrix for the organization of cells in complex structures. A well-designed, three dimensional scaffold is one of the fundamental tools to guide tissue formation in vitro and in vivo.

The role of the scaffold is to induce tissue regeneration by providing a "temporary guide" for cell growth, under appropriate culture condition, to facilitate the process of differentiation [9]. In this work we have focused mainly in the creation and analysis applications with bone grafting.

1.2.1. Properties of the scaffolds

Mechanical stability and specific biological compatibility are features of uttermost importance for tissue-engineering constructs. Consequently, we must consider two distinct sets of parameters during the design phase: biological parameters, related to the cells contacting the scaffold, and engineering parameters, related to the mechanical and micro structural features of the tissue to mimic. This affects the materials choice (natural or synthetic) especially in a bone-grafting context, so they will satisfy various requirements:

- ✓ Biocompatibility is necessary to avoid unwanted host tissue response to the implant. Biocompatibility is linked to the need of improving and/or restoring a specific biological function, without interfering or interacting in a harmful way with the physiological activity of the organism [10]. It is also understood that an ideal scaffold should promote vascular invasion within few weeks of implantation to actively support nutrient, oxygen and waste transport [11]. Beyond biocompatibility, bioactivity is seen as a plus. Scaffolds should mimic the structure and biological function

of the extracellular matrix; they should support ECM formation by promoting cellular function, and have the ability to provide biochemical signals to the cells. In the case of bone formation an ideal scaffold should also be able to recruit progenitor cells through bio-molecular signaling, a property known as osteoinduction.

- ✓ The materials used must show mechanical properties (elastic modulus, responses to applied loads) that are compatible with those of the replaced tissue. In vivo, the engineered structure should retain sufficient mechanical strength to tolerate any stress and physiological load imposed on it [12]. Mechanical properties of bone vary widely from cancellous to cortical bone. In particular, Young's modulus of cortical bone is between 15 and 20 GPa and that of cancellous bone is between 0.1 and 2 GPa. Compressive strength varies between 100 and 200 MPa for cortical bone, and between 2 and 20 MPa for cancellous bone. The large variation in mechanical property and geometry makes it difficult to design an ideal bone scaffold [13].

In addition to the basic material requirements, tissue engineering has also highlighted the importance of macro and micro structural properties of the scaffold. Some morphological properties play a crucial role on the survival, growth, diffusion and reorganization of cells. The properties of the scaffolds essential for cell growth are:

- ✓ High and interconnected porosity. The ideal scaffold must have a highly porous structure. Pores interconnection is a prerequisite

for a uniform cells distribution in space, their survival, proliferation and migration in vitro and it should as well provide the necessary space for the neo-vascularization of the surrounding tissue in vivo. High porosity and pores interconnection allow the use of bioreactors to create hydrodynamic microenvironments with a minimum number of constraints to the diffusion, which strongly reflect the fluid-dynamic conditions in vivo to obtain an extensive and well organized community of cells [12]. In an ideal scaffold pore size should be at least 100 μm in diameter for successful diffusion of essential nutrients and oxygen for cell survivability [14]. However, in bone tissue in-growth, pore sizes in the range of 100-150 and 150-200 μm are found to be optimum, while smaller pores (75-100 μm) resulted in ingrowth of un-mineralized osteoid tissue, and even smaller pores (10-75 μm) were penetrated only by fibrous tissue [15]. Conversely, a high porosity reduces the mechanical properties (e.g. compressive strength) and increases the complexity of scaffold manufacturing process.

- ✓ Bioresorbability is another crucial factor for scaffold in tissue regeneration. An ideal scaffold should be able to degrade with time in vivo, preferably at a controlled resorption rate and eventually creating space for the new bone tissue to grow. Naturally, designing and manufacturing multi-scale porous scaffolds having ideal composition including targeted biomolecules, mechanical properties and related bioresorbability

are some of the key challenges towards their successful implementation in tissue engineering.

1.2.2. Biomaterials used for scaffold fabrication

Polymeric materials most widely used in the biomedical field and, more specifically, in tissue engineering, can be natural or synthetic. The natural materials used [16] often have the advantage of specific cellular interactions, the so-called "cell recognition". These materials are either components of or have macromolecular properties similar to the natural ECM. However, the main issue concerning materials taken from human or animal tissues is their scarcity. The most natural materials used in tissue engineering are collagen, alginates, chitosan and hyaluronic acid (HA). Collagens are the main protein of mammalian tissue ECM and comprise 25% of the total protein mass of most mammals [17], [18]. Similarly, HA is found in varying amounts in all tissues of adult animals. HA, both alginate and chitosan are hydrophilic, linear polysaccharides [19]. They interact in a favorable manner *in vivo,* and thus have been utilized as hydrogel scaffold materials for tissue engineering [20]. Conversely, these materials have a limited versatility in scaffolds construction in terms of mechanical properties. In contrast, synthetic biopolymers offer an advantage over natural materials in that they can be industrially reproducible on a large scale. They can be also tailored to give a wide range of properties (in terms of structure and degradation rate) which are more predictable and

controllable. In particular, many investigations focused on synthetic biodegradable polymers that are already approved by the Food and Drug Administration (FDA). The main drawback of synthetic polymers is the lack of specific signals for cellular recognition. Synthetic polymers widely used in tissue engineering are biodegradable polyesters such as Polyglycolic Acid (PGA), Polylactic acid (PLA), Polycaprolactone (PCL). PCL consists of five non-polar methylene groups and a relatively polar ester group. The PCL degradation kinetics is very slow when compared to PLA, PGA. Consequently, it is suitable for long term sustained drug delivery extending over a period longer than one year [21]. The polyesters are relatively rigid materials and this is an advantage in load-bearing applications, and it is a disadvantage when mechanical continuity with the soft tissue or blood veins is required. Finally, none of these polyesters has chemically reactive functional groups for easy adhesion of drugs or biologically active media [12].

1.2.3. Techniques in scaffold fabrication

Several technologies have been developed to process synthetic and natural scaffold materials into porous structures. The techniques used depend on the polymer employed and the application of interest. To outline the state of the art, it first is necessary to distinguish between two different production approaches: namely “top-down” or “conventional techniques” and “bottom-up” or “non conventional techniques” (Table 1). Most commercially available

tissue engineering approaches are “top-down”, meaning that through a series of chemical or physical reactions it is possible to process a bulk material in order to obtain a given structure with certain characteristics. Traditional technologies include solvent casting, gas foaming, phase separation and many others.

Top- Down Techniques	Bottom-up Techniques
Solvent casting/ Particulate leaching	3D printing
Gas foaming	Stereolitography
Phase separation	Selective laser sintering (SLS)
electrospinning	Fused deposition model
	Microspheres sintering

Table.1 *Top-down and bottom-up techniques to fabrication scaffold*

However, scaffolds fabricated by these techniques do not adequately mimic the structure of the natural extracellular matrix in terms of architecture, which may be one of the reasons for suboptimal outcome in generating functional tissues In bottom-up approaches, scaffolds are fabricated assembling smaller building blocks. The unconventional techniques, also known as rapid prototyping (RP) or solid free-form fabrication (SFF), provide exceptional spatial control over the architecture of the polymer. They are based on the use of automated image processing systems that enable a computer-assisted design and fabrication, respectively

performed by CAD (computer-aided design) and CAM (computer-aided manufacturing). RP techniques can rapidly produce 3D objects using layer-by-layer manufacturing methods. They generally comprise the design of a scaffold modeled by using the CAD software that is subsequently broken down into a series of cross sections. For each cross section, a RP machine lays down a layer of material starting from the bottom and moving up a layer at time to create the scaffold. RP techniques are the most advanced techniques for scaffold fabrication. They can produce the parts with highly reproducible architecture and compositional variations. RP techniques have advantages over other fabrication techniques such as the ability to control matrix architecture (size, shape, interconnectivity, branching, geometry and orientation) yielding biomimetic structures varying in design and material composition. They also grant control over the mechanical properties and degradation kinetics of scaffold. One of the main drawbacks of these techniques is the trade-off between resolution and manufacturing speed achieved by current systems and a not so wide range of polymeric materials that can be used.

1.3. Importance of Growth Factors release in regenerative medicine

In order to overcome the difficulties of using artificial implants and organs transplantation, scientific research has focused his interest on regenerative medicine, leading to the formation of a new science

intersecting medical-biological skills and other disciplines related to engineering. The purpose of this multidisciplinary field is to restore the loss of physiological functions by replacing the organs and tissues diseased or damaged [8]. In the bone-grafting context, these pathological degenerations have been traditionally repaired utilizing autografts and allografts, because of their osteoconductivity, osteoinductivity and osteogenecity. Nonetheless their application is restricted because of donor shortage and donor-site morbidity [22] [23] as well as inconveniences associated with their transplantation such as immune rejection and pathogen transfer [24]. The branch of regenerative medicine known as Tissue Engineering (TE) was developed to overcome these limitations [25]. The National Science Foundation officially coined this term in 1988, indicating that the aim of this multidisciplinary field was to produce biological substitutes containing – or recruiting – living and functional cells for regeneration, maintaining or improving performance of the tissue [26]. Therefore TE integrates different disciplines such as medicine, biology, engineering and chemistry with the common aim of obtaining or replacing organs or parts of organs in the human body employing three fundamental "tools"; namely cells, scaffolds and growth factors (GFs) which, however, are not always simultaneously used [27]. On the other hand, recent experimental and clinical studies indicate that the success of any TE approach relies on the delicate and dynamic interplay among these three components and that functional tissue integration and regeneration depend upon their wise coordination [28]. Future generation scaffolds will have to provide not only the adequate mechanical and

structural support but also actively guide and control cell attachment, migration, proliferation and differentiation. This is in theory achievable if the scaffold function is extended to supply biological signals guiding and directing cell function thought a combination of matricellular cue exposition and GF sequestration and delivery [28]. A series of undesirable systemic effects such as toxicity, an insufficient local concentration and their rapid degradation is releated to the administration of the bolus of GF. Indeed, when a solution of the growth factor is injected into the site requiring regeneration, the biological effect cannot be always predicted. This is because the growth factor is rapidly diffused away from the injector site. To overcome the problem of *in vivo* instability, GFs are administered in polymeric vehicles to locally deliver the factor in a controlled, localized way for the desired time frame. Growth factors can be incorporated into the polymeric delivery systems in different ways, so the drug delivery systems (DDS) is able to enhance their activity [29]. It is possible that, when used in combination with an appropriate DDS technology, the growth factor enhances the *in vivo* proliferation and differentiation of key cells that promote tissue regeneration. It is possible to protect the growth factor against proteolysis, as it is incorporated in the release carrier for prolonged retention of the activity in vivo. DDS technology can be also useful for half-life prolongation, adsorption improvement and targeting, applicable in tissue engineering using protein and genes.

1.3.1. Type and mechanism of action

Growth factors are soluble macromolecules that define the biological environment. GFs are protein molecules specific for intercellular and cell-ECM signaling, which are involved in ECM dynamic properties through specific surface receptors, driving GFs regulatory activity [30]. Growth factor signaling starts up the specific cellular response of a very wide range of cell actions, including cell survival, and control over migration, differentiation or proliferation of a specific subset of cells. Initially the growth factor, which is secreted by the producer cell, goes to bind specific trans-membrane receptors on the target cells so to instruct cell behavior (Fig. 1). The machinery that traduces the growth factor-binding signal to the cell nucleus involves a complex array of events involving cytoskeleton protein phosphorylation, ion fluxes, changes in metabolism, gene expression, and protein synthesis and ultimately an integrated biological response [31]. Growth factors do not act in an endocrine fashion but differ from other oligo/polypeptide molecules, such as insulin and hormones, in the mode of delivery and response elicited. In fact, they exhibit short range diffusion through the extracellular matrix and act locally because of their short half-lives and slow diffusion. There are different ways to deliver particular signals of the growth factors that depend on not only their ability to diffuse though the extracellular matrix (ECM), but also depending on the target cell density, type of receptors that follow in an intracellular signals transduction. In this way, the same receptor can translate different messages depending

on the intracellular transduction pathways, which can differ from one cell type to another. The ultimate response of a target cell to a particular soluble growth factor can also be governed by external factors, including the ability of the factors to bind to ECM, ECM degradation and growth factors concentration and cell target location [29], [32].

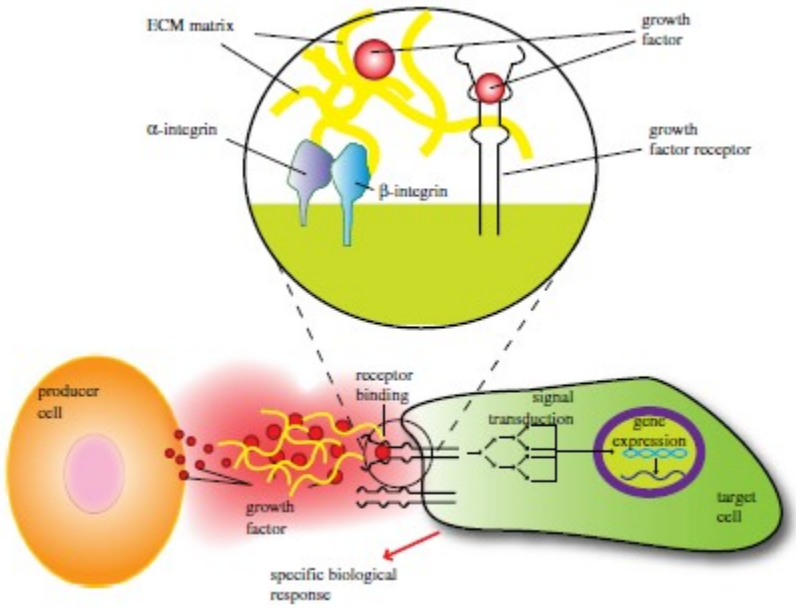

Figure.1 *Cross talks between cells mediated by growth factors and ECM. The producer cell secretes soluble growth factors that bind to target cell receptors. [33]*

1.3.2. Strategy for presentation of GF

There are several strategies we can pursue to control the release of growth factors from the scaffold, but some points should be considered first:

- ✓ The load capacity corresponds to the amount of growth factor that can be mixed into the scaffold;
- ✓ The distribution relates to the way the growth factor is dispersed, which will influence the release kinetics;
- ✓ The binding affinity defines how tightly a growth factor binds the system; this must be sufficiently low to allow release, but high enough to prevent uncontrolled release;
- ✓ The release kinetics: its control allows the appropriate dose of growth factor to reach the cells over a given period of time;
- ✓ The long-term stability: the system should enable growth factor to maintain their structure and activity over a prolonged period of time;
- ✓ The economical viability: such biomaterials must further be easy to manufacture and to handle, and be cost-competitive:

The strategies used in TE for growth factor presentation of biomaterial constructs are mainly two:

- Chemical immobilization of the growth factor into or onto the matrix;
- Physical encapsulation of growth factors in the delivery system [29].

Chemical methods have been investigated, but often result in the denaturation and activity lowering of protein because the functional groups of protein are chemically modified by immobilization reaction. Therefore, physical methods are preferable for growth factor integrity. In fact, such a physical immobilization is often observed in growth factors existing in the body [30]. Some growth factors are naturally stored in the body; they are stored ionically with the acidic polysaccharides of ECM (such as heparin sulfate and heparin) because most of them have a positively charged site on the molecular surface. It is widely accepted that, when needed, the complexed growth factor is water solubilized by the enzymes secreted from the surrounding cells released from the ECM complex during ECM degradation. This complexation also protects growth factors from their denaturation and general enzymatic degradation in vivo.

1.4. Time controlled in delivery system

In the field of pharmaceutical technology there are formulations that can release drugs in the body in amount and at controlled rates. It is possible to program the delay, the speed and the release of active molecules by numerous pharmaceutical forms. Those formulations are defined controlled drug delivery systems (DDS) that minimize unwanted side effects such as under or over dosing of drug. The use of this DDS can provide several advantages over traditional methods of administration, among them, DDS provide protection of

drugs, especially protein, that are otherwise rapidly destroyed by the body. Finally, DDS can increase patient comfort and compliance by replacing frequent (e.g., daily) doses with infrequent (once per month or less) injection. However, there are potential disadvantages that should not be overlooked. Possible toxicity of the materials used, dose dumping, requirement of surgical procedures to implant or remove the system, and higher manufacturing costs are disadvantages of using drug delivery system. DDS main advantage and disadvantage are summarized in Table 2. A large number of classes of drugs that include chemotherapeutic drugs, [34] immunosuppressant's, [35] anti-inflammatory agents, [36]-[37] antibiotics, [38]-[39] opioid antagonists, [40] steroids, [41]-[42] hormones, [43] can benefit from temporal or distribution controlled release.

DDS advantage	**DDS disadvantage**
Extension of the duration of actionand bioavailability of the drug	Possibility of toxivuty of the materials
Minimization of drug degradationand loss	Harmful degradation products
Preventionof drug's adverse side-effects	Necessity of sirurgical intervention either on systems application or removal
Reduction of dosin frequency	Patients disconfort with DDS device usage
Minimization of drug concentration fluctuations in pplasma level	High cost of final product
Improved drug utilization	
Improved patient compliance	

Table.2 *DDs advantage and disadvantage*

DDS can be produced by using natural or synthetic polymers, which can be biodegradable or non-biodegradable. (Table 3) These polymeric systems can be used in the release of drugs, protein and cells and they should present a set of properties that make them suitable materials to interact with the human body. One of the most important feature is biodegradability of the polymers, their degradation products should be normal metabolites of the body or products that can be metabolized and easily cleared from the body [44]-[45]. Moreover, synthetic polymers are used to develop new DDS with specific properties (chemical, interfacial, mechanical and biological) for a given application, simply by changing the building block or the preparation technique [46].

Drug	**Trade name**	**Company**	**Polymer**	**Roule**	**Application**
Buserelin acetate	Profact®depot suprefact® depot	Marion Roussel	PLGA	s/c implant	Prostate cancer
Goserelin acetate	Zoladex ®depot	AstraZeneca	PLGA	s/c implant	Prostate cancer, endometrioses
Lueprorelin acetate	Lupren®depot Enantone® depot trenantone ®	Takedia-Abbot	PLGA	3-mounth depot suspension	Prostate cancer, endometrioses
Octreotide acetate	Sandostatin LAR®depot	Novartis Pharma	PLGA	s/ suspension	GH suspension, anti cancer
triptorelin	Decapeptyl ®depot	Debiopharma	PLGA	Monthly s/c injection	LHRH agonist, prostate cancer

Table 3 *Example of protein-peptide controlled release systems based on PLGA*

1.5. PLGA- based drug delivery system

Poly(D,L-lactic-co-glycolide), PLGA (Figure.2) has shown immense advantages, among all the biodegradable polymers, as a drug delivery carrier and as scaffold material for tissue engineering [47]. These advantages include extended release rates (up to days, weeks or months) in addition to its biocompatibility/biodegradability and ease of administration. The American Food and Drug Administration (FDA) have also approved a very large number of drug delivery products based on this material [48]. PLGA or PLGA based nano/microcarriers can be successfully made to incorporate macromolecular drugs such as proteins, peptides, genes, vaccines, antigens, human growth factors, etc

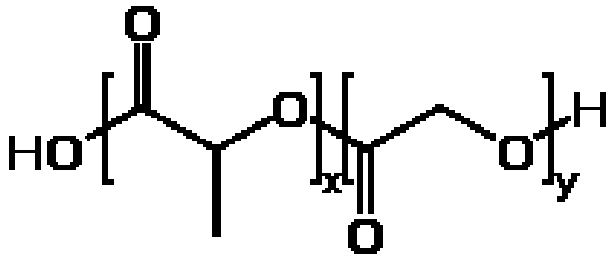

Figure.2 *PLGA Structure.*

Several benefits come from the possibility to control drug release adjusting various polymer parameters such as molecular weight, monomer ratio, drug loading, excipient loading, glass transition temperature, to name a few. This led to various medical and pharmaceutical applications. The advantage of using particle

systems include, in fact, the possibility of administering the medication directly to the site of action where the system forms a deposit from which the active molecules can be released and act for a prolonged period of time. Based on size, two different categories of carriers can be distinguished: microparticles and nanoparticles. The most accepted classification reports that particles up to 100 nm are considered nanoparticles while the ones from 1 μm up to 1,000 μm classified as microparticles. Their synthesis can be achieved from different techniques [49]. Emulsion polymerization, solvent evaporation, ionic gelation, self-assembly nanoprecipitation and supercritical fluid technology are some of them [50]. The mechanism of release by biodegradable polymeric microspheres consists of two stages: the diffusion of the drugs thought the polymer matrix and the biodegradation of the polymer matrix itself. An autocatalic bulk degradation process governs the release mechanism of active molecules from PLGA microspheres. This mechanism is affected by many physical and chemical factors, such as the initial pH, ionic strength and temperature of the external environment, the ratio of the copolymers, the molecular weight, the crystallinity and the size of species. In the diffusive-erosive mechanism an important role is played by the environment in which the drug is released. The particle, in contact with the aqueous environment hydrates, water getting inside solubilizes the drug that begins to spread through the macroporous structure of the PLGA microspheres. The presence of pores and their characteristics depend on the preparation techniques (e.g. multiple emulsion technique). The release of macromolecules can be prevented by the

microporosity of the system. Following the degradation of the polymer, micropores increase in size until the transport of the macromolecule can take place [51].

1.6. Protein and peptide in PLGA particles: instability and inactivation problems

The integrity of protein structures is essential for their function in physiological or pathological conditions, but both in vitro and in vivo many proteins, peptides are fragile molecules that undergo different pathways of instability, and they have limited half-life. For this reason they need to be carefully handled. Unexpected unfolding or degradation of a protein may lead to inactive, sometimes even toxic products. Protein instability, generally, can be divided into two chemical and physical processes. Chemical processes include hydrolysis (proteolysis), deamination, racemization, oxidation, disulfide formation and β-elimination, and involves the formation and destruction of covalent bonds, which usually occurs in the primary structure and disulfide bonds. Physical stability refers to proteins' ability to retain their secondary, tertiary and quaternary structure, which can be lost by reversible or irreversible denaturation through a loss of tertiary structure, aggregation and adsorption. A major issue, with PLGA delivery systems, is protein stability during preparation, storage and release. There are several factors associated with this polymer that may cause the destabilization of proteins [52]-[53]. During microspheres

preparation, protein are exposed to conditions that are known to cause denaturing and aggregation, namely high shear, elevated temperature, exposure to the air/liquid interface, organic solvents and the oil in water (O/W) interface. Higher energy emulsion methods such as by sonication, homogenization and vortex are detrimental to proteins [54]. The addition of an aqueous protein solution to an organic solvent can lead to protein denaturation. During release from polymer microparticles, proteins are exposed to many stresses that can compromise the physical and chemical stability of proteins. These include protein rehydration, exposure to soluble oligomers, low pH, interaction between protein and polymer, loss of stabilizing excipients, and physiological temperature. Interaction between protein and polymer, such as adsorption can also affect the stability of proteins. Adsorption occurs by a hydrophobic interaction between the polymer and the hydrophobic interior of proteins and can often lead to the formation of insoluble aggregates or irreversible conformational changes [55]. Even when adsorption is reversible, it may accelerate other deleterious reactions by exposing previously buried residues or increasing side chain mobility [56].

1.7. Stabilization strategies of growth factors in PLGA- based delivery systems

Several stabilizers have been shown to effectively improve protein stability in the polymer formulation DDS. However individual

proteins need to be carefully studied for better selection of stabilization strategies. Nonetheless, we can intervene on two fronts: during the preparation phase and /or during the release phase.

During preparation, the addiction of excipients, such as BSA [57] PEG 400 [58] and others, to the inner aqueous phase that compete with the water/organic solvent interface can prevent emulsification-induced denaturation and aggregation. This approach may be particularly useful when PLGA microparticles are loaded with low amounts of therapeutically potent proteins. On the other hand, increasing the protein concentration during emulsification was shown to result in higher absolute amounts of aggregated protein at the interface, indicating that multi-layer interfacial adsorption can occur [59]. Common surfactants have not been very successful as stabilizer in the emulsification step because they seem to have an insufficient competition with proteins for the water/organic solvent interface, or promotion of organic solvent/protein contacts through hydrophobic contacts with both components. Another approach to protect proteins against degradation during emulsification has been the pre-entrapment in a hydrophilic core, and is subsequently encapsulated in PLGA microparticles [60]. During the release phase specific stabilization approaches to minimize protein degradation associated with the direct environment of (degrading) PLGA are often needed. To inhibit the acid-induced degradation of proteins within the microparticles during the release (if they occur at all in vivo), co-incorporation of water poorly soluble salts of inorganic bases, such as magnesium hydroxide, calcium carbonate and

bicarbonate sodium is performed [61]. Finally, the addition of poloxamamers, such as Pluronics F68, induces a decrease in the interactions of the macromolecule with the free carboxyl residues of PLGA. [62]

References

1. Ferrara, N. and R.S. Kerbel, *Angiogenesis as a therapeutic target.* Nature, 2005. **438**(7070): p. 967-974.
2. Carmeliet, P., *Angiogenesis in life, disease and medicine.* Nature, 2005. **438**(7070): p. 932-6.
3. de Muinck, E.D. and M. Simons, *Re-evaluating therapeutic neovascularization.* Journal of Molecular and Cellular Cardiology, 2004. **36**(1): p. 25-32.
4. Patan, S., *Vasculogenesis and angiogenesis.* Cancer Treat Res, 2004. **117**: p. 3-32.
5. Carmeliet, P., *Mechanisms of angiogenesis and arteriogenesis.* Nat Med, 2000. **6**(4): p. 389-95.
6. Helisch, A. and W. Schaper, *Arteriogenesis: the development and growth of collateral arteries.* Microcirculation, 2003. **10**(1): p. 83-97.
7. Price, R.J., G.K. Owens, and T.C. Skalak, *Immunohistochemical Identification of Arteriolar Development Using Markers of Smooth-Muscle Differentiation - Evidence That Capillary Arterialization Proceeds from Terminal Arterioles.* Circulation Research, 1994. **75**(3): p. 520-527.
8. Ikada, Y., *Challenges in Tissue Engineering.* Tissue Engineering: Fundamentals and Applications, 2006. **8**: p. 423-462.
9. Schugens, C., et al., *Polylactide macroporous biodegradable implants for cell transplantation .2. Preparation of polylactide foams by liquid-liquid phase separation.* Journal of Biomedical Materials Research, 1996. **30**(4): p. 449-461.
10. Pietrabissa, R., *Biomateriali per protesi e organi artificiali.* Collana di Ingegneria Biomedica, 1996. **1**.
11. Burg, K.J., S. Porter, and J.F. Kellam, *Biomaterial developments for bone tissue engineering.* Biomaterials, 2000. **21**(23): p. 2347-59.
12. Leong, K.F., C.M. Cheah, and C.K. Chua, *Solid freeform fabrication of three-dimensional scaffolds for engineering replacement tissues and organs.* Biomaterials, 2003. **24**(13): p. 2363-78.

13. Olszta, M.J., et al., *Bone structure and formation: A new perspective.* Materials Science & Engineering R-Reports, 2007. **58**(3-5): p. 77-116.
14. Bose, S., M. Roy, and A. Bandyopadhyay, *Recent advances in bone tissue engineering scaffolds.* Trends in biotechnology, 2012. **30**(10): p. 546-554.
15. Hulbert, S.F., et al., *Potential of ceramic materials as permanently implantable skeletal prostheses.* J Biomed Mater Res, 1970. **4**(3): p. 433-56.
16. Bellamkonda, R., et al., *Hydrogel-based three-dimensional matrix for neural cells.* J Biomed Mater Res, 1995. **29**(5): p. 663-71.
17. Alberts, B., et al., *Differentiated cells and the maintenance of tissues.* Molecular biology of the cell, 3rd ed., Garland Publishing Inc, New York & London, 1994: p. 1139-1195.
18. Lee, C.H., A. Singla, and Y. Lee, *Biomedical applications of collagen.* Int J Pharm, 2001. **221**(1-2): p. 1-22.
19. Smidsrod, O. and G. Skjakbraek, *Alginate as Immobilization Matrix for Cells.* Trends in Biotechnology, 1990. **8**(3): p. 71-78.
20. Lee, K.Y. and D.J. Mooney, *Hydrogels for tissue engineering.* Chemical Reviews, 2001. **101**(7): p. 1869-1879.
21. Kweon, H., et al., *A novel degradable polycaprolactone networks for tissue engineering.* Biomaterials, 2003. **24**(5): p. 801-808.
22. Biermann, J.S., et al., *Metastatic bone disease: diagnosis, evaluation, and treatment.* J Bone Joint Surg Am, 2009. **91**(6): p. 1518-30.
23. Laurencin, C.T., et al., *Tissue engineering: orthopedic applications.* Annual review of biomedical engineering, 1999. **1**(1): p. 19-46.
24. Kretlow, J.D. and A.G. Mikos, *Review: mineralization of synthetic polymer scaffolds for bone tissue engineering.* Tissue Eng, 2007. **13**(5): p. 927-38.
25. Buck, B.E., T.I. Malinin, and M.D. Brown, *Bone transplantation and human immunodeficiency virus. An estimate of risk of acquired immunodeficiency syndrome (AIDS).* Clin Orthop Relat Res, 1989(240): p. 129-36.
26. Langer, R. and J.P. Vacanti, *Tissue engineering.* Science, 1993. **260**(5110): p. 920-6.

27. Biondi, M., et al., *Controlled drug delivery in tissue engineering.* Adv Drug Deliv Rev, 2008. **60**(2): p. 229-42.
28. Tabata, Y., *Significance of release technology in tissue engineering.* Drug Discovery Today, 2005. **10**(23-24): p. 1639-1646.
29. Mehta, M., et al., *Biomaterial delivery of morphogens to mimic the natural healing cascade in bone.* Advanced drug delivery reviews, 2012. **64**(12): p. 1257-1276.
30. Taipale, J. and J. KeskiOja, *Growth factors in the extracellular matrix.* Faseb Journal, 1997. **11**(1): p. 51-59.
31. Lamalice, L., F. Le Boeuf, and J. Huot, *Endothelial cell migration during angiogenesis.* Circulation Research, 2007. **100**(6): p. 782-794.
32. Cohen, G.B., R.B. Ren, and D. Baltimore, *Modular Binding Domains in Signal-Transduction Proteins.* Cell, 1995. **80**(2): p. 237-248.
33. Lee, K., E.A. Silva, and D.J. Mooney, *Growth factor delivery-based tissue engineering: general approaches and a review of recent developments.* Journal of the Royal Society Interface, 2011. **8**(55): p. 153-170.
34. Iwamoto, T., *Clinical Application of Drug Delivery Systems in Cancer Chemotherapy: Review of the Efficacy and Side Effects of Approved Drugs.* Biological & Pharmaceutical Bulletin, 2013. **36**(5): p. 715-718.
35. Martz, L., *Nanoparticles for lupus.* SciBX: Science-Business eXchange, 2013. **6**(11).
36. Bodmeier, R. and H. Chen, *Preparation and characterization of microspheres containing the anti-inflammatory agents, indomethacin, ibuprofen, and ketoprofen.* Journal of Controlled Release, 1989. **10**(2): p. 167-175.
37. Hickey, T., et al., *Dexamethasone/PLGA microspheres for continuous delivery of an anti-inflammatory drug for implantable medical devices.* Biomaterials, 2002. **23**(7): p. 1649-1656.
38. Prior, S., et al., *Gentamicin encapsulation in PLA/PLGA microspheres in view of treating Brucella infections.* International Journal of Pharmaceutics, 2000. **196**(1): p. 115-125.

39. Toti, U.S., et al., *Targeted delivery of antibiotics to intracellular chlamydial infections using PLGA nanoparticles.* Biomaterials, 2011. **32**(27): p. 6606-6613.
40. Saez, V., J.R. Hernández, and C. Peniche, *Microspheres as delivery systems for the controlled release of peptides and proteins.* Biotechnologia Aplicada, 2007. **24**: p. 108-116.
41. Ishihara, T., et al., *Efficient encapsulation of a water-soluble corticosteroid in biodegradable nanoparticles.* International journal of pharmaceutics, 2009. **365**(1): p. 200-205.
42. Oh, Y.J., et al., *Preparation of budesonide-loaded porous PLGA microparticles and their therapeutic efficacy in a murine asthma model.* Journal of controlled release, 2011. **150**(1): p. 56-62.
43. Kim, H.K., H.J. Chung, and T.G. Park, *Biodegradable polymeric microspheres with "open/closed" pores for sustained release of human growth hormone.* Journal of Controlled Release, 2006. **112**(2): p. 167-174.
44. Nair, L.S. and C.T. Laurencin, *Polymers as biomaterials for tissue engineering and controlled drug delivery*, in *Tissue engineering I*. 2006, Springer. p. 47-90.
45. Pillai, O. and R. Panchagnula, *Polymers in drug delivery.* Current Opinion in Chemical Biology, 2001. **5**(4): p. 447-451.
46. Coelho, J.F., et al., *Drug delivery systems: Advanced technologies potentially applicable in personalized treatments.* The EPMA journal, 2010. **1**(1): p. 164-209.
47. Makadia, H.K. and S.J. Siegel, *Poly Lactic-co-Glycolic Acid (PLGA) as Biodegradable Controlled Drug Delivery Carrier.* Polymers, 2011. **3**(3): p. 1377-1397.
48. Mundargi, R.C., et al., *Nano/micro technologies for delivering macromolecular therapeutics using poly(D,L-lactide-co-glycolide) and its derivatives.* Journal of Controlled Release, 2008. **125**(3): p. 193-209.
49. Pinto Reis, C., et al., *Nanoencapsulation I. Methods for preparation of drug-loaded polymeric nanoparticles.* Nanomedicine, 2006. **2**(1): p. 8-21.
50. Lee, L.Y., C.H. Wang, and K.A. Smith, *Supercritical antisolvent production of biodegradable micro- and nanoparticles for controlled delivery of paclitaxel.* J Control Release, 2008. **125**(2): p. 96-106.

51. Batycky, R.P., et al., *A theoretical model of erosion and macromolecular drug release from biodegrading microspheres.* J Pharm Sci, 1997. **86**(12): p. 1464-77.
52. Bilati, U., E. Allémann, and E. Doelker, *Strategic approaches for overcoming peptide and protein instability within biodegradable nano-and microparticles.* European Journal of Pharmaceutics and Biopharmaceutics, 2005. **59**(3): p. 375-388.
53. Giteau, A., et al., *How to achieve sustained and complete protein release from PLGA-based microparticles?* International journal of pharmaceutics, 2008. **350**(1): p. 14-26.
54. Sah, H., *Stabilization of proteins against methylene chloride water interface-induced denaturation and aggregation.* Journal of Controlled Release, 1999. **58**(2): p. 143-151.
55. Van Tassel, P.R., et al., *A particle-level model of irreversible protein adsorption with a postadsorption transition.* Journal of Colloid and Interface Science, 1998. **207**(2): p. 317-323.
56. Prior, S., et al., *Gentamicin encapsulation in PLA/PLGA microspheres in view of treating Brucella infections.* International Journal of Pharmaceutics, 2000. **196**(1): p. 115-125.
57. Nihant, N., et al., *Polylactide Microparticles Prepared by Double Emulsion-Evaporation .2. Effect of the Poly(Lactide-Co-Glycolide) Composition on the Stability of the Primary and Secondary Emulsions.* Journal of Colloid and Interface Science, 1995. **173**(1): p. 55-65.
58. Péan, J.-M., et al., *Why does PEG 400 co-encapsulation improve NGF stability and release from PLGA biodegradable microspheres?* Pharmaceutical research, 1999. **16**(8): p. 1294-1299.
59. Sah, H., *Protein instability toward organic solvent/water emulsification: Implications for protein microencapsulation into microspheres.* Pda Journal of Pharmaceutical Science and Technology, 1999. **53**(1): p. 3-10.
60. Lee, H.K., J.H. Park, and K.C. Kwon, *Double-walled microparticles for single shot vaccine.* Journal of Controlled Release, 1997. **44**(2-3): p. 283-293.

61. Agrawal, C.M. and K.A. Athanasiou, *Technique to control pH in vicinity of biodegrading PLA-PGA implants.* Journal of Biomedical Materials Research, 1997. **38**(2): p. 105-114.
62. Blanco, M.D. and M.J. Alonso, *Development and characterization of protein-loaded poly(lactide-co-glycolide) nanospheres.* European Journal of Pharmaceutics and Biopharmaceutics, 1997. **43**(3): p. 287-294.

Chapter 2

2. Material and methods

2.1. Induction of angiogenesis in 3D scaffolds for bone regeneration

2.1.1. Vascularization in early bone regeneration

Bone formation and development occur through two distinct processes: intramembraneous and endochondral ossification [63] in which vascularization plays a key role. In intramembranous bone formation, in fact, the matrix is deposited by mature osteoblasts, which differentiate from mesenchymal stem cells (MSCs) transported through capillaries. Osteoblasts play an important role in the balance of resorption and the deposition of bone matrix by secreting osteoprotegerin that is an inhibitor molecule of osteoclast activity [64]. On the other hand, during the endochondral ossification, the chondrocytes secret angiogenic growth factors promoting the invasion of blood vessels, which then bring along a number of highly specialized cells and replace the cartilage mold with bone and bone marrow [65]. Successively blood vessels transport osteoprogenitor cells for the deposition of new bones and endhotelial cells of blood vessels produce growth factors that control the recruitment, proliferation, differentiation and function of various cells including osteoblasts and osteoclast [66] [67]. The vasculature, thus, plays an important role both as a reservoir of bioactive signals necessary for bone morphogenesis [68] and as a conduit for the recruitment of essential cells involved in bone remodeling. During bone development the balance between

cartilage formation and vascular invasion is of fundamental importance as any change in this balance leads to growth plate thickening and a reduction in bone formation.

2.1.2. The role of VEGF in bone regeneration: neo-vascularization

During the processes of development, remodeling and repair of bone tissue, VEGF plays a crucial role in the phase of vascularization. This growth factor is produced by endothelial cells, macrophages, fibroblast, smooth muscle cells, osteoblasts and hypertrophic chondrocytes and during bone regeneration it is active both directly and indirectly on osteoblats differentiation. Directly, VEGF promotes migration, proliferation and differentiation of osteoblasts, and plays also a mediating role for different osteoinductive factors, such as TGF, IGF-I and FGF-2, which up-regulate VEGF expression in osteoblasts [69, 70]. VEGF acts also indirectly on osteoblats by stimulating endothelial cells, and producing anabolic factors that improve the bone formation [71]. In neo-vascularization, VEGF drives the processes of angiongenesis and arteriogenesis by its mitigenic and chemotactic effects and facilitates the recruitment of circulating endothelial progenitor cells. During angiogenesis EC migration and proliferation start under the effect of VEGF that causes immature tube-like structures to branch from mature blood vessels and if this signal is removed, these nascent vessels regress. Because VEGF has a half-life of 90 min

once introduced into a host environment, it is important to provide an adequate exposure to VEGF to induce a cellular response [72]. VEGF is a 46-kDa glycoprotein that comprises six related proteins: VEGF-A, VEGF-B, VEGF-C, VEGF-D, VEGF-E and the placenta growth factor. The most studied member of the VEGF family is VEGF-A. This family exists in different isoforms derived from the same gene by alternative splicing of messenger RNA and defined on the basis of the length of the amino acids chain, such as VEGF121, VEGF165, VEGF189, and VEGF209 in humans [73]. VEGF-A is considered the prototype member in the family, it is the predominant factor in the regulation of angiogenesis and endothelial cell growth. Similar to most peptide growth factors, VEGF binds to the extracellular domain of two tyrosine kinase receptors on the cell surface of its target : VEGFR-1 or fsm-like tyrosine kinase 1 (Flt-1) and VEGFR-2 or fetal liver kinase 1 (Flk-1) also known as kinase-insert domain-containing receptor (KDR). VEGF bind induces receptor dimerization and autophosphorylation of the intracellular kinase domain. The phosporylated tyrosines are docking sites for the assembly of multiprotein complexs that start different intracellular cascade, ending up in endothelial cell activation. Whereas the role of VEGF-1 is still under debate, it is well known that VEGFR-2 phosporilation stimulates ECS proliferation, migration and survival. It is the predominant factor in the regulation of angiogenesis and endothelial cell growth.[74]

2.1.3. The role of VEGF- mimetic peptide QK in vascularization

Because of the important role VEGF plays in angiogenesis, it is considered an important target in the pharmacological. The x-ray structure of the complex VEGF/flt-1 d2 shows that the binding interface is mainly localized in three regions. One of them is the α-helix crossing the amino acid sequence 17-25. This region contains some of the key residues involved in receptors recognition, so a well designed helical peptide represents a tractable target for peptide engineering [75]. QK is a linear peptide of 15 amino acids, (Acetyl-KLTWQELYQLKYKGI-Ammide) which should interact with the VEGF receptors - an important prerequisite for its biological activity. The presence of amino acids with intrinsic helix preference gives QK its helical fold and on opposite faces of the peptide there is an amphipathic feature of the helix, which allows a number of medium range ionic, polar and hydrophobic interactions. Moreover, QK peptide, which is composed by only 15 amino acids, could represent a model for further studies [76] (see Fig. 3). In fact, this peptide induces attachment and proliferation of endothelial cells and promotes their activation and capillary like formation in vitro [77] [76]. In vivo, QK peptide has also shown some therapeutic promise, it has mostly been used as a locally delivered soluble factor [78]. To improve its activity, QK peptide has been immobilized on inorganic substrates [77] and self assembling peptide scaffolds [79], but also conjugated to bioactive hydrogels [80] and to hydroxypatite through a binding peptide [80].

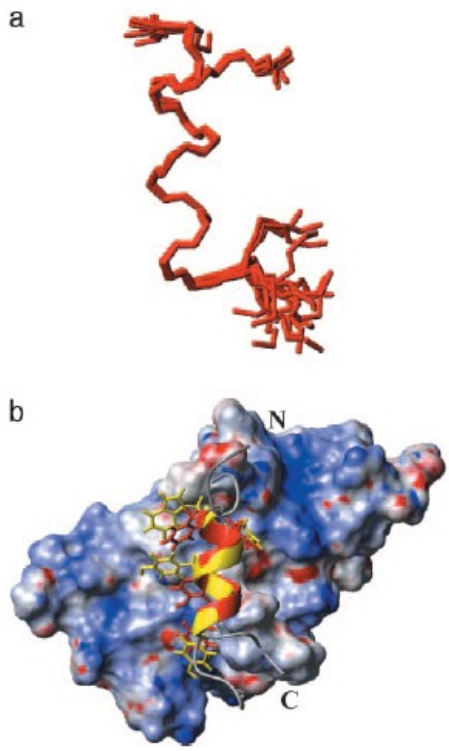

Figure.3 *NMR structure of QK. (a) Superposition of the backbone of the best 20 CYANA QK structures. (b) Backbone superposition of the QK representative structure (yellow) and VEGF helix (red) bound to Flt-1D2. Side chain of the interacting residues and the Flt-1D2 electrostatic surface are shown [76]*

2.2. Scaffold for bone regeneration

2.2.1. Bottom-up approach for tridimensional scaffold realization

During the design of scaffolds it is important to gain accurate control over their macroscopic properties (i.e., geometry, mechanical strength, density, porosity), microstructural ones (e.g., size, interconnection of the pores) and on their bioactivation (surface functionalization, release of growth factors). For this purpose there are several techniques that depend on the type of polymer used and the application intended. In recent years, many studies focused on the development of porous scaffolds by sintering of polymeric microparticles in order to overcome several limitations found in conventional techniques, mainly related to the mechanical properties, pore interconnection, as well as the use of toxic solvents. For this reason, in this work we propose a bottom up approach based on the assembly of building blocks by solvent induced microparticles sintering to realize multifunctional polymer scaffolds with predefined pore dimensions. This approach gives an extra degree of freedom since it is possible to include - inside the construct - an array of microdepots for the release of bioactive molecules. Scaffolds manufactured this way show controlled microstructure, chemical stability and a mechanical response necessary to support neo-tissue growth. The possibility of presenting bioactive agents in a predefined chrono-programmed

manner is a feature that can give the promising capability of guiding cells and tissue processes.

Polymeric microsphere sintering is achieved by partial dissolution of the microspheres surface to form porous three-dimensional structures. Two boundary cases limit the process and can be clearly underlined: an initial state in which particles come in contact and a final situation in which the pores are utterly closed in a continuous matrix. We can obtain a porous material only stopping the process between the first and the second stage. This can be done only with an accurate control of the process parameters. The use of specific solvent/non solvent mixtures under mild temperatures was exploited to overcome some limitations intrinsic to thermo labile bioactive molecules, such as growth factors, which tend to denaturate with temperature. The Flory-Huggins solution theory models the interplay between monomer-monomer and monomer-solvent interaction in a polymer:solvent mixture.

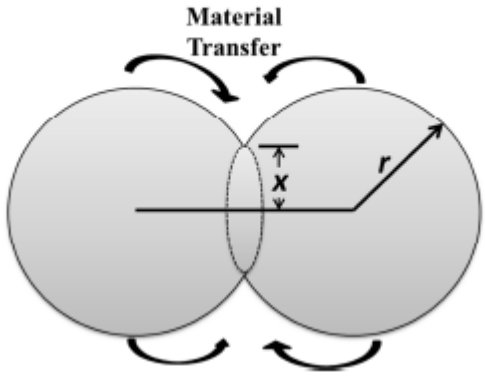

Figure.4 *Representation of a junction point formed between two beads in contact*

With a specific solvent/non-solvent mixture it is possible to balance between polymer dissolution and precipitation. During the dissolution step a microsphere can develop bonds with adjacent microspheres [81]. (Figure.4)

2.2.2. Scaffold obtained by microspheres sintering

For their regeneration, different tissues require different microenvironments, but usually an optimum porosity is a common prerequisite. Regarding the regeneration of bone tissue, it is important for scaffolds to have an appropriate pore size in a range from 200 to 400 μm [82]. Based on literature data, the present work focused on the realization of three dimensional structures with pores size around 200 um. In order to build a scaffold with such characteristic, we used a simple geometric model to calculate the right diameter range of the microspheres used (see Fig.5). In this model, four rigid spheres of equal diameter are arranged symmetrically along the diagonals of the square in which they are inscribed.

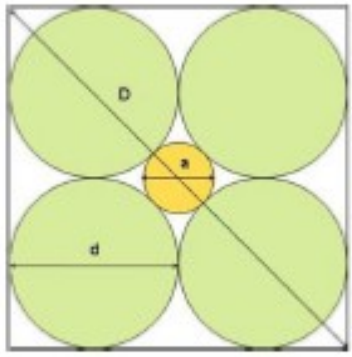

***Figure.5**-Spheres model schematization*

The characteristic dimension of the cavity between the four spheres can be approximated by the diameter of the rigid sphere inscribed in it:

$$\frac{D - 2d}{2} = \alpha$$

Where: D is the diagonal of the square in which spheres are inscribed, d is the initial diameter of the rigid spheres. By simple geometric considerations, and based on the available sieves dimensions (see Section 2.4) microspheres in the 455-500 μm diameter range were used to obtain a pore size of around 200 μm.

2.3. Materials

The acid poly (D, L-lactic-co-glycolic acid) (PLGA) 50:50 (Resomer® RG 504H, i.v. 0:32 to 0:44 dl/g) was purchased from Evonik® (Germany). The poloxamer188 (Pluronic ® F68, Mw 8400, HLB 29), the Poly(ε-captolactone) (PCL)(Mw=65kDa), the polyvinyl alcohol (Mowiol 40-88)(Mw=13-23 kDa) and phosphate buffer (0.01M Na_2HPO_4, 0.0027 M KCl and 0.137 M NaCl, pH 7.4) were purchased from Sigma Aldrich (USA). Dicklorometane and chloroform were purchased from Romil Pure Chemistry (Cambridge, GB). PDMS SYLGARD 184 (PolyDimethylSiloxane) was purchased from Dow Corning (Germany). All solvents used are of analytical grade and HPLC grade and were supplied by Sigma Aldrich (USA). The water used was filtered through 0.22 μM filter (Millipore, USA). Protected N-Fmoc-amino acid derivatives, acetic anhydride, coupling reagents and Rink amide MBHA resin have been purchased from Novabiochem. DIPEA is provided from Applied Biosystem. All other reagents are commercially available from Sigma-Aldric and all solvents are commercially available from LabScan.

2.4. Scaffold assembly

2.4.1. Polycaprolactone Microparticles

The PCL microparticles were prepared by the technique of oil in water (O⁄W) single emulsion with solvent evaporation. Briefly, a polymer solution, obtained by dissolving the polycaprolactone in dichloromethane(50 ml, 10% w⁄v), is added dropwise into 100ml of a aqueous PVA solution (Mowiol ® 40-88) with 0.1% of Tween 21. The presence of such emulsifying agents in the aqueous phase is essential for reducing the phenomena of coalescence and aggregation of the microspheres during the evaporation of the solvent. The two solutions are mixed for three hours at a speed of 400 rpm, using an electronic stirrer (RZR 2102, Heidolph,Germany), so as to allow the complete evaporation of volatile organic solvent and in order to obtain the dispersed microparticles. After, these microparticles are filtered and washed three times with distilled water to remove the emulsifying agents, and finally allowed to dry under a chemical hood.

2.4.2. Monolayers

PCL microspheres sieved in the selected size range (455–500 μm) were processed into a PDMS alignment mold made up of an array of PDMS pillars.

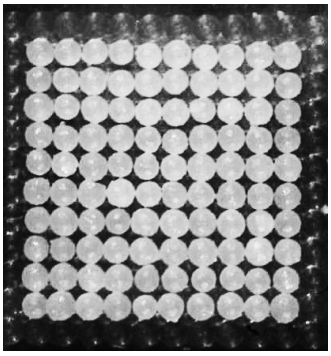

Figure.6 *PCL microspheres micro-posizioned in PDMS mold*

Each individual microsphere has its own accommodation in this kind of structure and four other adjacent microspheres border it. These alignment structures allow the arrangement of PCL microspheres in layers – or arrays - of 10x10 elements (Fig.6). Successively, a solvent (100% anisole) was poured over the microspheres (just a drop of 50 μL). The solvent sintering solution was immediately rinsed with ethanol - a PCL non-solvent - and allowed to evaporate from the sintered microspheres.

2.4.3. 3D ordered scaffold

After the creation of monolayers of PCL microspheres, obtained by solvent sintering, another alignment structure shaped as a box was used to put them in an ordered stack and sinter them together. The result is a scaffold in which microspheres are arranged in a 3-dimensional simple cubic lattice. The alignment mold prevents slippage between adjacent layers and provides a complete correspondence between the microspheres of adjacent layers. The

samples were processed with three different solvent/non-solvent concentrations, in order to evaluate their mechanical properties during the compression test. The concentrations used are shown in the following Table.4. In each case, the solvent/non solvent sintering solution was immediately rinsed with ethanol as non solvent and allowed to evaporate from the sintered microspheres. All microspheres appear sintered together with fully formed interconnecting *necks*.

Anisole-Ethanol
30%-70%
50%-50%
70%-30%

Table.4 *Three different solvent concentrations anisole/ethanol for the last step of ordered 3D scaffold sintering*

2.4.4. Qualitative and quantitative analysis: X-ray microtomography (micro-CT)

A qualitative and quantitative evaluation of the scaffolds obtained was carried out by 3D image analysis using a computerized microtomograph, SkyScan1172 (Bruker). Microtomography (commonly known as Industrial CT Scanning), like tomography, uses X-rays to obtain projection images of a 3D-object that later can be processed to obtain a virtual tomografic model made up of several cross-sectional images of the object under test. MicroCT technique was performed in order to evaluate scaffolds morphology: the

optimized processing conditions lead to sintered microspheres scaffolds with a well defined three-dimensional microstructure. It was also performed in order to quantify the pore size, pore volume and overall percentage of interconnected porosity of the sintered matrices. Each voxel of a micrograph represents the absorption degree of X-radiation in an elementary volume. To assess scaffolds porosity in the reconstructed images, it is necessary to discriminate between air and the absorbing material, a step known as binarization. Binarization is carried out by imposing a threshold on the absorption spectrum of these images. The result of this operation is a binary image (0/1 W/B) in which the black and white voxels represent respectively the empty volume and the one occupied by PCL. It is up to the software then, to count white and black voxels, obtaining the object-to-void volume ratio and hence porosity.

2.5. Surface treatment

Surface hydrophobicity has a great influence on cell response *in vivo* and *in vitro*. As many works show [83, 84] the more hydrophilic is the surface of a material, the better cell adhesion on that surface will be. Moreover, cell adhesion, spreading and proliferation is improved when some serum proteins (like fibronectin and vibronectin in culture medium and/or from secretion [85, 86]) are preferentially adsorbed on the material surface. PCL, which was extensively used in this work, is a semi crystalline linear polyester, and surely possesses suitable features for tissue

engineering application, such as biodegradably, biocompatibility, mechanical strength and flexibility [87]. Nevertheless, its low surface wettability, due to its rather high hydrophobicity, adversely affects cell attachment and proliferation. In fact, when the cellular suspension is placed on top of a porous PCL scaffold the culture medium is not adsorbed, resulting in a low initial cell seeding density, heterogeneous cell distribution and slow cell growth [88]. Several surface treatments are available in order to increase the surface hydrophilicity of polyesters, and thus improve cell-material interfacing, cell adhesion and enhance cell proliferation and functions [89]. Among them, there are temporary treatments such as *pre-wetting* in which the hydrophobic porous polymer scaffold is easily pre-wetted in ethanol, which is then exchanged with the culture medium. During this treatment there is no change on the inherent hydrophobic character of polymer. Another temporal method is *plasma treatment* that can provide a reactive chemical environment even on inert surfaces, and change the surface properties creating desired functionalities for further polymer grafting onto the surface [90]. Finally, *Surface NaOH hydrolysis* can be considered. This technique uses strong alkali conditions (1M NaOH acqueos solution) to improve the hydrophilicity of polymeric scaffold by the hydrolysis of the ester group (-COOH) of polymer to carboxylic acid and hydroxyl group.

We have modified the surface of the scaffold by two different treatments:

a) hydrolysis of the surface witch Ethanol\0.1N NaOH mix solution (15min, 200 RPM) to increase the percentages of hydroxyl (–OH) and carboxylic acid (–COOH) groups on the surface area.

b) O_2 plasma treatment. The plasma treatment was carried out on a Gmbh Plasma Deposition System (Model Femto Diener, 13.53 Mhz, DE) under O_2 at 20%. The chamber was evacuated to less than 10 Pa before filling with oxygen. After the pressure of the chamber had stabilized to a proper value, glow discharge plasma was created by controlling the electrical power at a radio frequency of 13.56 MHz for a predetermined time (1min).

2.5.1. Water contact angle test

To study the effect of different treatments on the surface of bioactive scaffolds, static contact angle measurements were performed. The contact angle is the angle, conventionally formed by the meeting of a liquid-vapor interface with solid liquid interface and it quantifies the wettability of a solid surface by a liquid. The surface wetting characteristics were examined with a drop-shape analysis system. Deionized water droplets (~ 2 μL) were delivered to the sample surface by a syringe at room temperature and the droplet configuration was captured with a camera. From the measured angle between the droplet baseline and the tangent at the water/air boundary, a contact angle was calculated as the average of the measured left and right contact angles. For statistical analysis 3

contact angle measurements were obtained from three different surface regions of three identical samples.

2.5.2. Mechanical characterization

In vitro release studies of QK from sintered scaffolds were made by suspending one scaffold in 100 µL of PBS pH 7.4 previously filtered through filter pores of 0.22 µm in diameter (Millex®, Millipore, USA). The samples were incubated in an incubator at 37 ° C and 50 rpm, to mimic the in vivo conditions. At regular intervals of time, the release media removed and replaced with the same volume of fresh PBS pH 7.4. The samples taken were analyzed by (Q-TOF) LC-MS, to determine the amount of peptide released. The results were expressed as µg of QK released per scaffold ± standard deviation (SD) of the measurement carried out on five different batches.

2.5.3. Cells adhesion test on scaffold surface treated

Specific tests were carried out to evaluate the influence of the two surface treatments on the process of cell adhesion. Scaffolds (untreated, plasma and EtOH/NaOH treated) were placed in a 96 multiwell plate and seeded with human umbilical endothelial vein cells (HUVECs) suspended in medium in order to obtain a surface

concentration of $9*10^3$ cells/cm^2. The different scaffolds were then placed in an incubator at 37° C with a controlled atmosphere at 5% CO2. After 72 h of incubation cells adhered to different scaffolds were counted through the Burker chamber. The number of cells that were located on the bottom of the container or in suspension was subtracted to the plated cells total, giving the number of cells who actually adhered to the scaffolds.

To observe cell morphologies, part of the scaffolds seeded with cells, were fixed 72 h after seeding, in 2.5% glutaraldehyde (SIC, Rome, Italy), 0.1 M sodium cacodylate (SIC), pH 7.3. They were subsequently washed three times for 10 min in the same buffer, post-fixed in 1% osmium tetroxide (SIC), 0.1 M sodium cacodylate, pH 7.3, on ice for 1 hour, washed three times for 10 min in the same buffer and dehydrated in ascending series of ethanol on ice. At the end of dehydration, samples were put in critical point drying (CPD Leica) placed on an aluminum stub with carbon tape, coated with 20 nm of gold metal by sputter coating (208 HR sputter coater Cressington) and observed with a Zeiss ultraplus scanning electron microscopy.

2.6. QK peptide synthesis and characterization

The sequence KLT WQE LYQ LKY KGI of QK peptide was synthesized by solid phase peptide synthesis as C-terminally amidated and N-terminally acetylated derivates following standard

Fmoc chemistry protocol on a fully automated multichannel peptide synthesizer Biotage® Syro Wave™. Rink-amide resin (substitution 0.45 mmol/g) was used as solid support. Coupling for each amino acid involves the following steps:

-Deprotection of the N-terminal function (2 steps by 10 min) with a solution to a 30% Piperidine in DMF;

-Coupling of 10 equivalent of Fmoc-AA, 9,9 equivalent of HOBT/HBTU (0,45 M solution in DMF) and 20 equivalent of DIPEA (2 M solution in NMP) compared with 0.1 mmol scale synthesis;

Three washes with DMF for 1 min were performed after each module. Acetylation was carried out with two treatment of 5 min with appropriate volume of a solution of acetic anhydride (2 M)/DIPEA (O.55 M)/ HOBt (0.06 M). Cleavage from solid support was performed by treatment with a TFA/TIS/water (95:2, 5:2, 5, v/v/v) mixture for 2 hours at room temperature. Crude peptide was precipitated in cold diethyl-ether, dissolved in a water/acetonitrile (9:1, v/v) mixture and lyophilized. Preparative purification of synthetic peptides has been carried out on a RP-HPLC, (Waters 2535 Quaternary Gradient Module), equipped with a 2489 UV/Visible detector applying a linear gradient of acetonitrile (0, 1% TFA) from 20% to 80% in 20 min at flow rate of 7 mL/min. Peptide eluted at 41 % of acetonitrile concentration. The column used was an X-Bridge^{TM} BEH300 preparative 10× 100 mm C18, 5µm column. Peptide purity and identity were confirmed on an Agilent 6530 Accurate-Mass Q-TOF LC/MS spectrometer with a gradient

of acetonitrile (0.1% Formic Acid) from water (0.1 % Formic Acid) of 5% to 60% in 7 min. The column used was the Symmetry C18 3.5µm column (4.6 × 75 mm, Phenomenex, Torrance, CA, USA.). To obtain an accurate analysis by Total Ion Current chromatogram (TIC) an Extracted Ion Chromatogram (EIC) was extracted for $[M+H^{3+}]/3$ = 651.7060 ± 0,5000 Da to obtain an area related only to the chemical species of interest.

2.7. Reference peptide (RP) synthesis and characterization

The sequence KGYLQTWILKEKL of RP peptide was synthesized by solid phase peptide synthesis as C-terminally amidated and N-terminally acetylated derivates following standard Fmoc chemistry protocol on a fully automated multichannel peptide synthesizer Biotage® Syro Wave™. Rink-amide resin (substitution 0.45 mmol/g) was used as solid support. Coupling for each amino acid involves the following steps:

-Deprotection of the N-terminal function (2 steps by 10 min) with a solution to a 30% Piperidine in DMF;

-Coupling of 10 equivalent of Fmoc-AA, 9,9 equivalent of HOBT/HBTU (0,45 M solution in DMF) and 20 equivalent of DIPEA (2 M solution in NMP) compared with 0.1 mmol scale synthesis;

Three washes with DMF for 1 min were performed after each module. Acetylation was carried out with two treatment of 5 min

with appropriate volume of a solution of acetic anhydride (2 M)/DIPEA (O.55 M)/ HOBt (0.06 M). Cleavage from solid support was performed by treatment with a TFA/TIS/water (95:2, 5:2, 5, v/v/v) mixture for 2 hours at room temperature. Crude peptide was precipitated in cold diethyl-ether, dissolved in a water/acetonitrile (9:1, v/v) mixture and lyophilized. Preparative purification of synthetic peptides has been carried out on a RP-HPLC, (Waters 2535 Quaternary Gradient Module,) equipped with a 2489 UV/Visible detector applying a linear gradient of acetonitrile (0, 1% TFA) from 20% to 80% in 20 min at flow rate of 7 mL/min. Peptide eluted at 39 % of acetonitrile concentration. The column used was an X-Bridge^{TM} BEH300 preparative 10× 100 mm C18, 5µm column. Peptide purity and identity were confirmed on an Agilent 6530 Accurate-Mass Q-TOF LC/MS spectrometer with a gradient of acetonitrile (0.1% Formic Acid) from water (0.1 % Formic Acid) of 5% to 60% in 7 min. The column used was the Symmetry C18 3.5µm column (4.6 × 75 mm, Phenomenex, Torrance, CA, USA.). To obtain an accurate analysis by Total Ion Current chromatogram (TIC) an Extracted Ion Chromatogram (EIC) was extracted for $[M+H^{3+}]/3 = 554.3330 \pm 0{,}5000$ Da to obtain an area related only to the chemical species of interest.

2.8. PLGA microparticles for controlled release of QK

2.8.1. PLGA microparticles synthesis

PLGA-Poloxamer and PLGA microspheres containing QK were prepared by the technique of multiple emulsion/solvent evaporation (W/O/W). A sterile solution in water (250 µl) containing QK, was emulsified by homogenization at 8000 rpm for 1 minutes (Ultraturrax T25 Basic, probe 8G, IKA, Germany), in a solution of 2,5 ml of PLGA and poloxamer 188 (5:1 ratio) or only PLGA polymer in dichloromethane (10% w/v). The emulsion obtained was added to the external phase consisting of 100 ml of an aqueous PVA solution (1.5% w/v) (Mowiol® 40-88) and emulsified by an electronic stirrer (RZR 2102, Heidolph, Germany) at 450 rpm for 3 hours, at room temperature, in order to facilitate the evaporation of the organic solvent and the precipitation of the polymer in the form of microparticles. Thereafter, microparticles were isolated and washed with 30 ml of distilled water 3 times, by centrifugation at 5000 rpm for 10 minutes at 4^0C, and subsequently subjected to a lyophilization cycle of 24 hours (0,001 atm , -60°C) (Freeze Dryer Alpha 1-4 LD plus, Martin Christ, DE).

2.8.2. Morphological analysis: Scanning electron microscopy observation

The morphology and internal structure of the microspheres was visualized using scanning electron microscopy (SEM) (Zeiss, FEG Ultraplus, Germany). A small quantity of plain microspheres was sprinkled on the SEM stubs and coated using a SEM coating system (Cressingthon, 208 HR, UK) with 10nm of platinum-palladium under an argon atmosphere. Samples surface morphology was then observed and photographs were taken at 20000 Kv and different magnification.

2.8.3. QK Encapsulation efficiency

The amount of QK encapsulated within the microspheres was determined by degradation of the polymeric system. Briefly, 2 mg of microspheres were dissolved into 200 µl of Ethyl Acetate and QK was extracted into 100 µl of water. The suspension was maintained at room temperature for about 4 hours in agitation at 400 rpm. The obtained solution was centrifuged at 15 rpm for 1 min and the QK peptide content in the aqueous phase as analyzed by (Q-TOF) LC-MS. The results were expressed as encapsulation real or actual loading (µg QK encapsulate for mg of microspheres) and encapsulation efficiency (µg encapsulated real QK/ QK theoretical

X100) ± Standard deviation (SD) of the measurement carried out on five different batches.

2.8.4. QK in vitro release kinetics

In vitro release kinetics of QK peptide were made by suspending 2 mg of lyophilized microspheres in 100 µl of PBS Ph 7.4 previously filtered through filter pores of 0.22 µm in diameter (Millex®, Millipore, USA). The samples were incubated in an incubator at 37 °C and 50 rpm, to mimic the condition of release of the microspheres dispersed in a scaffold. At regular intervals of time, the sample were centrifuged at 300 rpm for 5 minutes at 4°C and the release media removed and replaced with the same volume of fresh PBS pH7.4. The samples taken were analyzed by (Q-TOF) LC-MS, to determine the amount of peptide released. The results were expressed as µg of QK released per mg of microparticles ± (SD) of the measurements carried out on five different batches.

2.8.5. Bioactive scaffold "In Vitro" Release kinetics

In vitro release studies of QK from sintered scaffolds were made by suspending one scaffold in 100 µL of PBS pH 7.4 previously filtered through filter pores of 0.22 µm in diameter (Millex®, Millipore, USA). The samples were incubated in an incubator at 37

° C and 50 rpm, to mimic the in vivo conditions. At regular intervals of time, the release media removed and replaced with the same volume of fresh PBS pH 7.4. The samples taken were analyzed by (Q-TOF) LC-MS, to determine the amount of peptide released. The results were expressed as μg of QK released per scaffold ± standard deviation (SD) of the measurement carried out on five different batches.

2.8.6. In vitro sprouting angiogenesis assay

Human Umbilical Vein Endothelial Cells (HUVECs) (Lonza) were grown in Medium 200 supplemented with LSGS kit (Life-Technologies) at 37°C in 5% CO_2 and 100% relative humidity (RH). At early passages (II-IV) they were employed in order to generate endothelial spheroids. After 3-4 days of culture, confluent HUVECs monolayers were trypsinized and 800 cells per spheroid were suspended in culture medium containing 0.25% (w/v) carboxymethylcellulose (Sigma), seeded into ultra-low-attachment round-bottom 96-well plates (Costar) and cultured as described to allow spheroids formation. After 24 h spheroids were harvested, centrifuged at 900 rcf for 15 minutes, suspended in 1.2mg/ml bovine skin collagen, transferred in 48-well plates (Falcon) and incubated. Once collagen polymerized M 200 culture medium supplemented with 2% FBS and 1% Pen Strep (10,000 U/mL penicillin G sodium, and 10,000 μg /mL streptomycin sulphate in 0.85% saline) (Gibco) was added.

The proangiogenic activity of QK released from PLGA microspheres with or without poloxamer co-encapsulation at different QK concentrations was evaluated. A dose-response assay was performed in order to test the release aptitude of the depots as well as the bioactivity of the encapsulated peptide in 24h. In particular the concentrations of QK tested were 40, 80, and 160 ng/ml. Briefly the amount of QK was calculated according to encapsulation efficiency of two formulations of microspheres and the final concentration of peptide to be tested. (40 80 and 160 ng/ml). To know the number of microspheres able to release the exact concentration of QK, after 24h, the calculated amount of peptide was divided by the dose of QK/single microsphere. (μg QK/mg microspheres divided number of microspheres contained in 1 mg, which is about 300 microparticles for microspheres of 200-300 μm).

Moreover, free QK released after 24h by a number of microspheres loaded in order to provide a presumed released peptide amount of 40 ng/ml was tested. PLGA-poloxamer and PLGA microspheres were suspended in 100 μL of PBS at pH 7.4 previously filtered using a 0.22 μm pores filter. The samples were then incubated at 37 °C and 50 rpm. After 24h the supernatant was removed and added to the spheroids culture medium.

Spheroids were divided into four groups of eight samples each. Groups were identified and treated as follows: positive control (QK 40 ng/ml), negative control (basal medium), QK released from microspheres embedded in collagen and from microspheres

suspended in PBS. Spheroids were then incubated at 37°C, with 5% CO2, and 100% RH.

After a 24h culture, gels were observed by an inverted light microscope before being fixed with 4% paraformaldehyde for at least 40 minutes, rinsed with PBS buffer and stained with Phalloidin tetramethylrhodamine B isothiocyanate (Sigma-Aldrich) and Sytox green (Invitrogen) for actin microfilaments and cellular nuclei respectively. Sprouting was evaluated by a Leica SP5 confocal laser scanning microscope using a HCX APO LU-V-l 10.0 X 0.30 water objective lens. Samples were excited with a 488 nm argon laser for nuclei detection while for actin a 543nm He–Ne laser was employed. A 560–600 nm or a 505–530 nm emission was used to detect actin and nuclei respectively. Images processing and quantitative analysis were performed by Leica LAS AF Version 2.7.3.9723 software.

References

1. Clarkin, C.E., et al., *Evaluation of VEGF-mediated signaling in primary human cells reveals a paracrine action for VEGF in osteoblast-mediated crosstalk to endothelial cells.* Journal of cellular physiology, 2008. **214**(2): p. 537-544.
2. Marx, R.E., *Bone and bone graft healing.* Oral Maxillofac Surg Clin North Am, 2007. **19**(4): p. 455-66, v.
3. Chung, U.-i., et al., *Distinct osteogenic mechanisms of bones of distinct origins.* Journal of Orthopaedic Science, 2004. **9**(4): p. 410-414.
4. Zhou, J., et al., *The repair of large segmental bone defects in the rabbit with vascularized tissue engineered bone.* Biomaterials, 2010. **31**(6): p. 1171-1179.
5. Barou, O., et al., *Relationships between trabecular bone remodeling and bone vascularization: a quantitative study.* Bone, 2002. **30**(4): p. 604-612.
6. Brandi, M.L. and P. Collin-Osdoby, *Vascular biology and the skeleton.* Journal of bone and mineral research, 2006. **21**(2): p. 183-192.
7. Goad, D., et al., *Enhanced expression of vascular endothelial growth factor in human SaOS-2 osteoblast-like cells and murine osteoblasts induced by insulin-like growth factor I.* Endocrinology, 1996. **137**(6): p. 2262-2268.
8. Wang, D.S., et al., *Increase of vascular endothelial growth factor mRNA expression by 1, 25-dihydroxyvitamin D3 in human osteoblast-like cells.* Journal of Bone and Mineral Research, 1996. **11**(4): p. 472-479.
9. Gerber, H.-P. and N. Ferrara, *Angiogenesis and bone growth.* Trends in cardiovascular medicine, 2000. **10**(5): p. 223-228.
10. Ennett, A.B., D. Kaigler, and D.J. Mooney, *Temporally regulated delivery of VEGF in vitro and in vivo.* Journal of Biomedical Materials Research Part A, 2006. **79**(1): p. 176-184.
11. Robinson, C.J. and S.E. Stringer, *The splice variants of vascular endothelial growth factor (VEGF) and their receptors.* Journal of Cell Science, 2001. **114**(5): p. 853-865.

12. Lemmon, M.A. and J. Schlessinger, *Cell Signaling by Receptor Tyrosine Kinases.* Cell, 2010. **141**(7): p. 1117-1134.
13. Olsson, A.K., et al., *VEGF receptor signalling - in control of vascular function.* Nat Rev Mol Cell Biol, 2006. **7**(5): p. 359-71.
14. Holmes, K., et al., *Vascular endothelial growth factor receptor-2: structure, function, intracellular signalling and therapeutic inhibition.* Cell Signal, 2007. **19**(10): p. 2003-12.
15. DeGrado, W.F., et al., *De novo design and structural characterization of proteins and metalloproteins.* Annu Rev Biochem, 1999. **68**: p. 779-819.
16. D'Andrea, L.D., et al., *Targeting angiogenesis: structural characterization and biological properties of a de novo engineered VEGF mimicking peptide.* Proc Natl Acad Sci U S A, 2005. **102**(40): p. 14215-20.
17. Zhang, K., A. Sugawara, and D.A. Tirrell, *Generation of Surface-Bound Multicomponent Protein Gradients.* ChemBioChem, 2009. **10**(16): p. 2617-2619.
18. Dudar, G.K., et al., *A vascular endothelial growth factor mimetic accelerates gastric ulcer healing in an iNOS-dependent manner.* American Journal of Physiology-Gastrointestinal and Liver Physiology, 2008. **295**(2): p. G374-G381.
19. Ravichandran, R., M. Griffith, and J. Phopase, *Applications of self-assembling peptide scaffolds in regenerative medicine: the way to the clinic.* Journal of Materials Chemistry B, 2014.
20. Leslie-Barbick, J.E., et al., *The promotion of microvasculature formation in poly (ethylene glycol) diacrylate hydrogels by an immobilized VEGF-mimetic peptide.* Biomaterials, 2011. **32**(25): p. 5782-5789.
21. Brown, J.L., L.S. Nair, and C.T. Laurencin, *Solvent/non-solvent sintering: A novel route to create porous microsphere scaffolds for tissue regeneration.* Journal of Biomedical Materials Research Part B: Applied Biomaterials, 2008. **86**(2): p. 396-406.
22. Robinson, B.P., et al., *Calvarial Bone Repair with Porous D,L-Polylactide.* Otolaryngology-Head and Neck Surgery, 1995. **112**(6): p. 707-713.

23. Goddard, J.M. and J. Hotchkiss, *Polymer surface modification for the attachment of bioactive compounds.* Progress in polymer science, 2007. **32**(7): p. 698-725.
24. Xu, L.C. and C.A. Siedlecki, *Effects of surface wettability and contact time on protein adhesion to biomaterial surfaces.* Biomaterials, 2007. **28**(22): p. 3273-83.
25. Arima, Y. and H. Iwata, *Effects of surface functional groups on protein adsorption and subsequent cell adhesion using self-assembled monolayers.* Journal of Materials Chemistry, 2007. **17**(38): p. 4079-4087.
26. Hanson, A.D., et al., *Effects of oxygen plasma treatment on adipose-derived human mesenchymal stem cell adherence to poly(L-lactic acid) scaffolds.* J Biomater Sci Polym Ed, 2007. **18**(11): p. 1387-400.
27. Woodruff, M.A. and D.W. Hutmacher, *The return of a forgotten polymer—polycaprolactone in the 21st century.* Progress in Polymer Science, 2010. **35**(10): p. 1217-1256.
28. Lee, J.H., et al., *Interaction of Different Types of Cells on Polymer Surfaces with Wettability Gradient.* J Colloid Interface Sci, 1998. **205**(2): p. 323-330.
29. Yildirim, E.D., et al., *Enhanced cellular functions on polycaprolactone tissue scaffolds by O2 plasma surface modification.* Plasma Processes and Polymers, 2011. **8**(3): p. 256-267.
30. Grace, J.M. and L.J. Gerenser, *Plasma treatment of polymers.* Journal of Dispersion Science and Technology, 2003. **24**(3-4): p. 305-341.

Chapter 3

3. Results and discussion

3.1. 3D Ordered Scaffolds: fabrication and morphological characterization

The first step, which consists in the assembly of monolayers from single microspheres, is crucial for the fabrication of a design compliant 3D scaffold as much as the following stacking of multiple monolayers. It is also important to underline here that only a standardized ordered structure can have highly predictive mechanical and morphological properties along with the possibility of integrating precise functional elements (e.g. depots of biological factors) dispositions.

As previously shown, PCL microspheres obtained by single emulsion-evaporation technique were arranged neatly on PDMS molds in order to obtain monolayers by chemical sintering with a solution of solvent-non-solvent for the PCL (Anisole / Ethanol). Shortly after pouring pure solvent - used for ease of implementation - ethanol was added to stop the swelling and control the process. The solvent caused the swelling of microspheres and connecting necks between them were subsequently formed. In all cases, necks were uniform (see Fig. 7).

The next step was a multilayer structure sintering. The sintered 3D Ordered Scaffolds were built by stacking individual layers inside a Teflon box-shaped mold (l=5x5 mm , h=1,5 mm) and sintering them once again with a solution at a different concentration of solvent-non solvent, to ensure all necks formation between the microspheres.

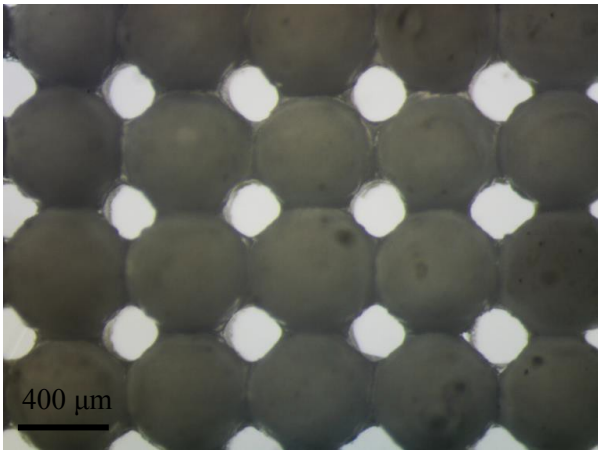

Figure.7 *Magnification of necks obtained by sintering with anisole 100%*

Compared to the first step, a further sintering with pure solvent (anisole 100%) would lead to polymer structure collapse.

In order to avoid local collapses and /or pores occlusion is important to have more control on the swelling. The concentrations used are shown in Table 5. The effect of solvent concentration (% Anisole/% Ethanol) on scaffold morphology was evaluated by Micro-CT scanning. Based on the outcome of this measurement It was possible to optimize the processing conditions and obtain scaffolds with a well defined three-dimensional microstructure.

The results are shown in Fig. 8, which depicts the effect of the concentration of the sintering solution on the degree of sintering between the microspheres.

Anisole-Ethanol
70%-30%
50%-50%
30%-70%

Table.5 *Three different solvent (anisole/ethanol) concentrations for the last step of ordered 3D scaffold sintering*

Scaffolds sintered at 50%-50% and 70%-30% v/v Anisole/Ethanol, show partial occlusions in the porous network. In the case of sintering with a solution 30%-70% v/v Anisole/Ethanol, the microscopic analysis indicated that microspheres are packed together with a precise geometry and connecting necks are arranged uniformly and isotropically. The scaffold porosity is highly interconnected.

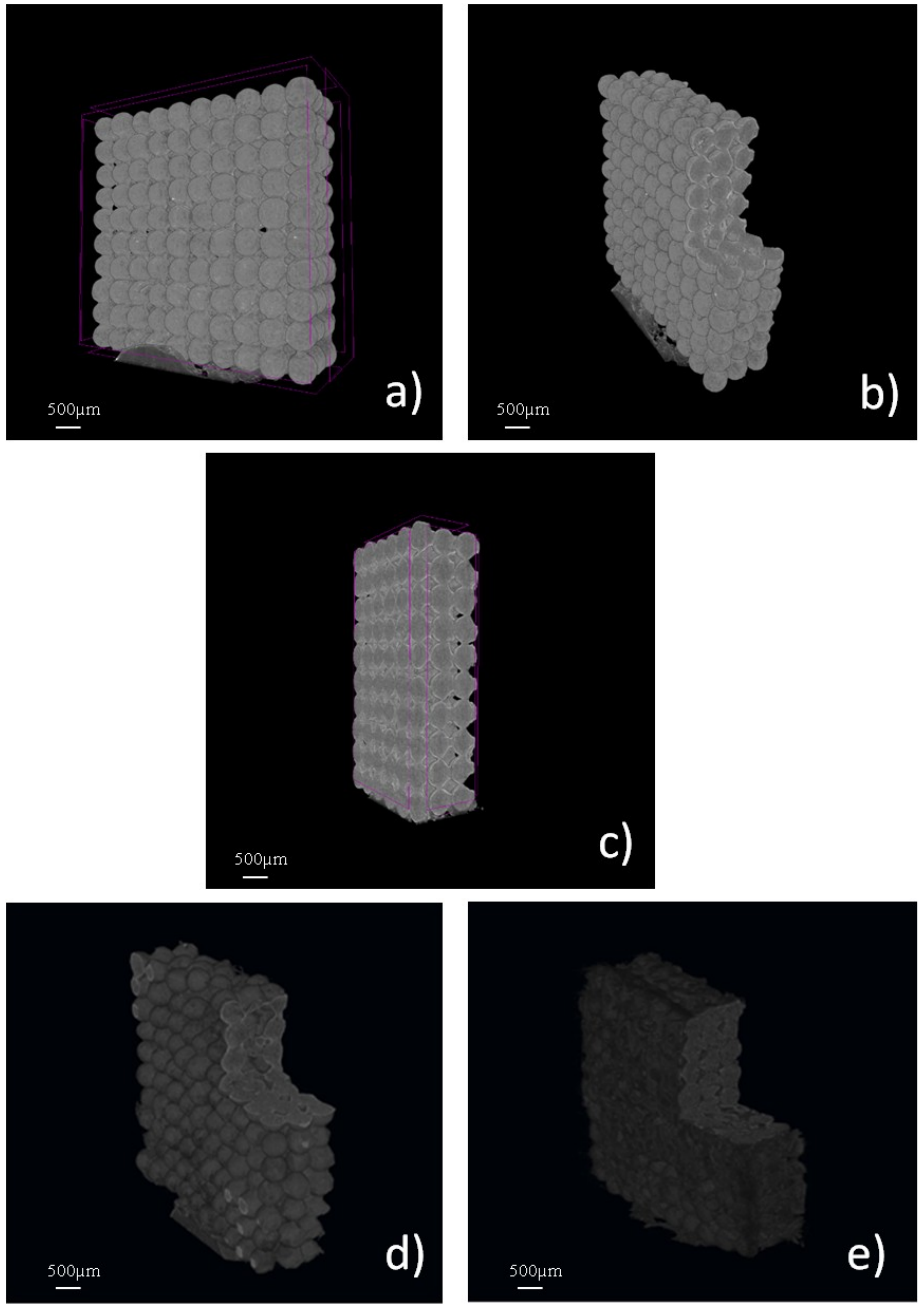

Figure.8 *Section micrographs of 3D ordered scaffold; a), b), c) Anisole/ethanol 30:70 (v/v); d) Anisole/ ethanol 50:50 (v/v); e) Anisole/ ethanol 70:3 (v/v)*

3.2. Porosimetric MicroCT analysis

To evaluate both qualitatively and quantitatively the degree of porosity, scaffolds pore size and volume and overall percentage of interconnected porosity were measured by a 3D image analysis of microCT tomographic scans. As explained in Chapter 2, each voxel in a 3D micrograph represents the X-ray absorption degree in the elementary volume. To assess scaffolds porosity, a binarization of the reconstructed images is therefore necessary; the black voxels will correspond to the empty volume. The software counts the white and black voxels, and the measurement of porosity is straightforward. This technique allows evaluating the pore size distribution or the interconnection degree, replacing more common – and less reliable - techniques such as mercury porosimetry. Scaffold porosity was compared with the theoretical porosity, using a simple geometrical model. If we consider a simple cubic unit cell for the microsphere lattice, each vertex of the cell contains 1/8 of microsphere, for a total volume occupation of one single microsphere. In this simple cubic lattice model, the edge of the cube is therefore equal to 2 times the radius of a microsphere.

Porosity is a scalar quantity and it is generically defined as the ratio between the volume of voids and the total volume of the material considered. In the specific case of a simple cubic disposition of spheres it can be calculated by the following equation:

$$\frac{(V_C - V_S)}{V_C} = \frac{(2r)^3 - \frac{4}{3}\pi r^3}{(2r)^3} = 1 - \left(\frac{1}{8}\frac{4}{3}\pi\right) = 0.48$$

Where: $V_C = l^3 = (2r)^3$ is the volume of the cube and $V_S = 4/3(\pi r^3)$ is the sphere volume.

Therefore 48% is the theoretical 3D scaffold porosity for a cubic disposition of microspheres, in accordance with the value measured by micro-CT scans analysis.

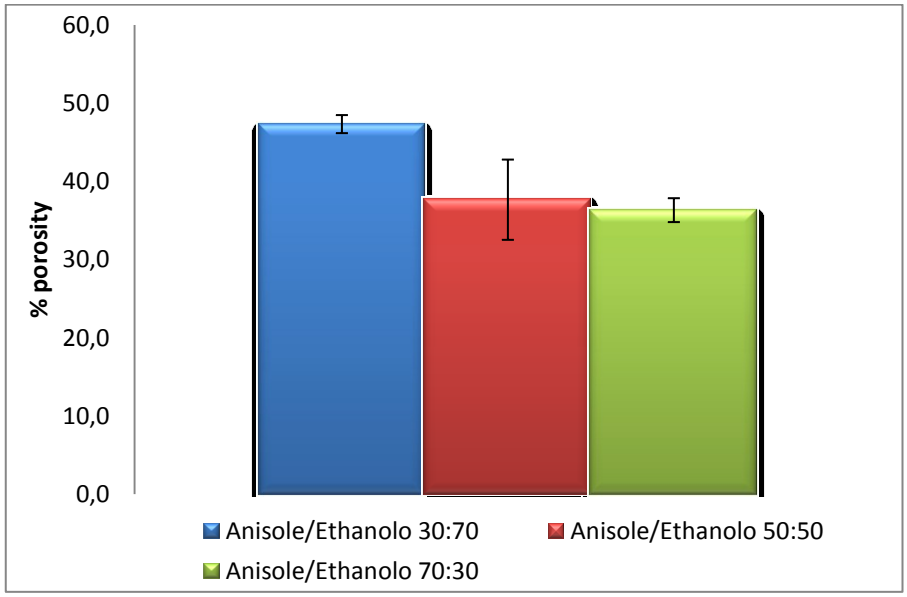

Figure.9 *Effect of solvent Anisole on the scaffold porosity*

The results in Fig. 9, show that the total porosity decreases from 48 to 36% with increasing anisole concentration. The use of a high anisole concentration increases the swelling phenomenon of PCL microspheres. From a qualitative analysis of the microtomographic images it is possible to observe that scaffold porosity and the degree

of interconnection reduce because of the presence of irregular *necks* in the structure.

3.3. Mechanical properties

The mechanical strength of the sintered scaffolds, as well as the influence of Anisole solvent on the sintering process, was evaluated by mechanical compression tests. Test results are reported in Table 6.

Scaffold type	Solvent/non solvent concentration
ORDERED SCAFFOLD	30%-70%
	50%-50%
	70%-30%

Table.6 *Type of samples tested in different solvent-non solvent concentration*

Stress-strain curves gave information on some of the mechanical properties of the constructs. Compressive modulus was evaluated for each sample from the slope of the linear region of the stress–strain curve. Then, compressive modulus of each scaffold type was calculated as the average of same-type samples. The graph in Fig.10 compares the compressive moduli of each scaffold type.

.

.

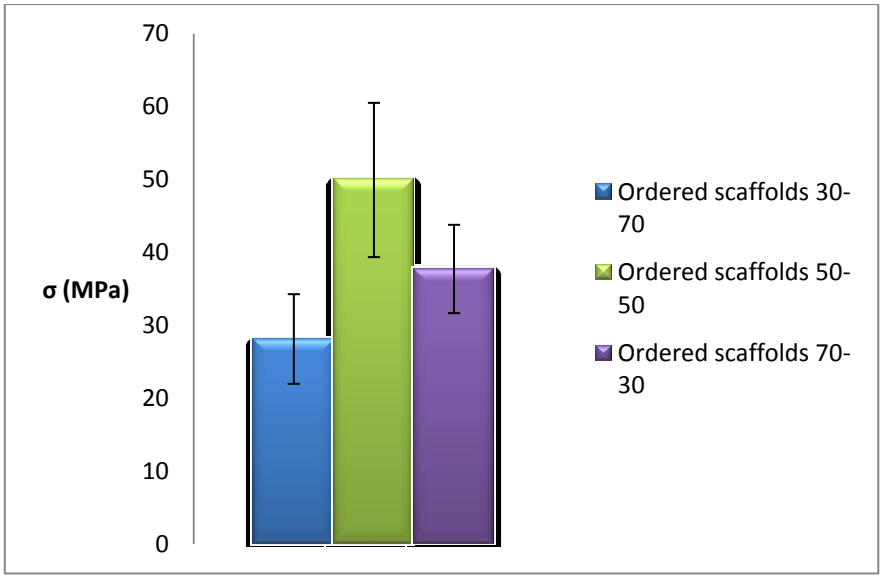

Figure.10 *Compressive modulus of scaffold at different Anisole/ Ethanol (v/v) concentration*

The results show that a change in solvent concentration has a significant effect on the elasticity of the polymeric 3D ordered scaffolds. Ordered scaffolds processed with a higher solvent concentration have a greater elastic modulus. This could be justified by the fact that when concentration increases, also the fraction of PCL that dissolves increases, filling the structure pores.

Compressive mechanical properties of some PCL scaffolds manufactured through other fabrication techniques are reported in literatue [91]. According to Eshraghi et al., the compressive mechanical properties of bulk and porous PCL specimens were measured. Reported here, for bulk PCL, the mean compressive modulus was 299–317.1 MPa and the mean 0.2% offset yield strength was 10.3–12.5 MPa. While for 3D ordered scaffold

obtained by SLS technique and with a porosity of about 80%, compressive modulus was 15 MPa [92]. The compressive moduli of human trabecular bone range from 1 to 5000 MPa and the ultimate compressive strength ranges from 0.1 to 27.3 MPa [93] [94]. Thus, the order of magnitude of the elastic moduli of all the scaffolds types fabricated is consistent with that reported in literature and fall within the lower range of values reported for human trabecular bone.

3.4. Surface treatments

The surface properties of a material and the degree of hydrophilicity or hydrophobicity in particular play a very important role in cell adhesion during the initial period of cell seeding. This determines the successful formation of tissue constructs leading to the subsequent cell proliferation, differentiation and new tissue in-growth. Because scaffolds are composed of PCL, a highly hydrophobic polymer, to facilitate the process of cell adhesion and proliferation they were subjected to two types of treatments: chemical and plasma treatments A morphological, mechanical and biological characterization of all these constructs was performed in order to compare them and underline their differences and benefits.

To study the effect of the different treatments, the water contact angles on scaffolds surfaces were measured by a sessile drop technique, previously described. Conventionally if water contact

angle is smaller than 90° the solid surface is considered hydrophilic whereas if water contact angle is larger than 90° the solid surface is considered hydrophobic. Therefore, 2μL of water were deposited above every scaffold sample and measurements were carried out at three different time points:

- At the moment the drop is deposited on the surface (0 seconds);

- At an intermediate time (15 seconds);

- A sufficiently long time to consider the drop as well positioned (30 seconds).

The results obtained for each treated scaffold and for the untreated ones are showed in Table 7.

TIME (s)	UNTREATED SCAFFOLD	NaOH TREATMENT	PLASMA TREATMENT
0	104,06	67,25	64,29
15	102,83	0	0
30	102,70	0	0

Table.7 *Measured static contact angle data at different time point on untreated, NaOH/EtOH treated and plasma treated PCL scaffold surface.*

The values in Table 8 show that untreated scaffolds have an angle greater than 90° for every time point, since the material is hydrophobic. It is also possible to observe that the drop deposited above the untreated samples remains on the surface and is not absorbed over time (Figure.11).

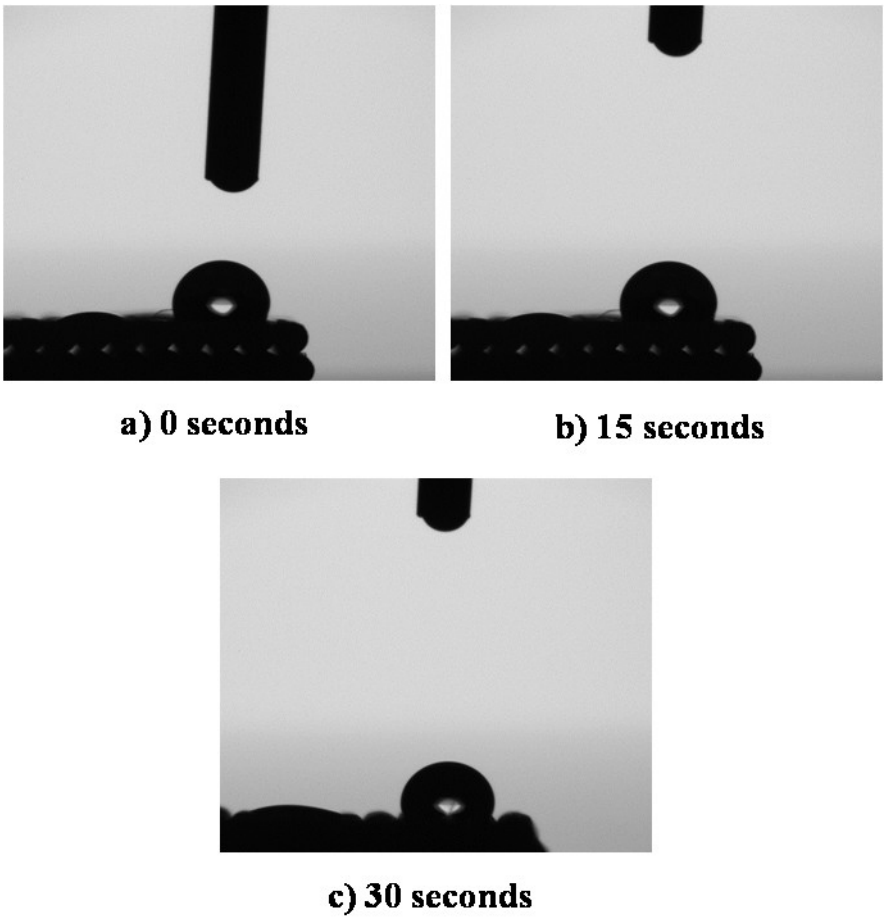

Figure.11 *a), b), c) Water contact angle images at different time point on untreated scaffold;*

PCL becomes hydrophilic after the surface treatments as suggested by the measured angle. In these cases, the only frames that it was possible to obtain are those at zero seconds, or rather those obtained as soon as the drop has been deposited (Figure.12) because after a few milliseconds the droplet is completely absorbed

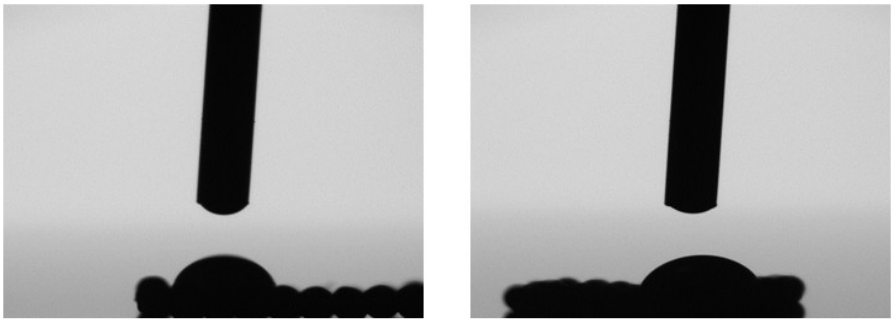

Figure.12 *d) water contact angle on plasma treated scaffold, e) water contact angle on NaOH treated scaffold*

These results show clearly that both treatments are able to increase polymer wettability. Plasma surface modification and Ethanol/ sodium hydroxide treatments enhance the presence of polar functional group that not only increase the surface wettability of the polymer but also improve early cell attachment and protein adsorption.

To confirm this hypothesis treated surfaces were also analyzed by scanning electron microscopy (SEM). Micrographs of NaOH treated 3D scaffolds show (Fig. 13) a more rippled surface compared to the control. While on the scaffolds treated with plasma, an increase in corrosion degree on the surface is noticeable

Increasing surface roughness should inversely decrease the contact angle of water and, therefore, improve the hydrophilicity.

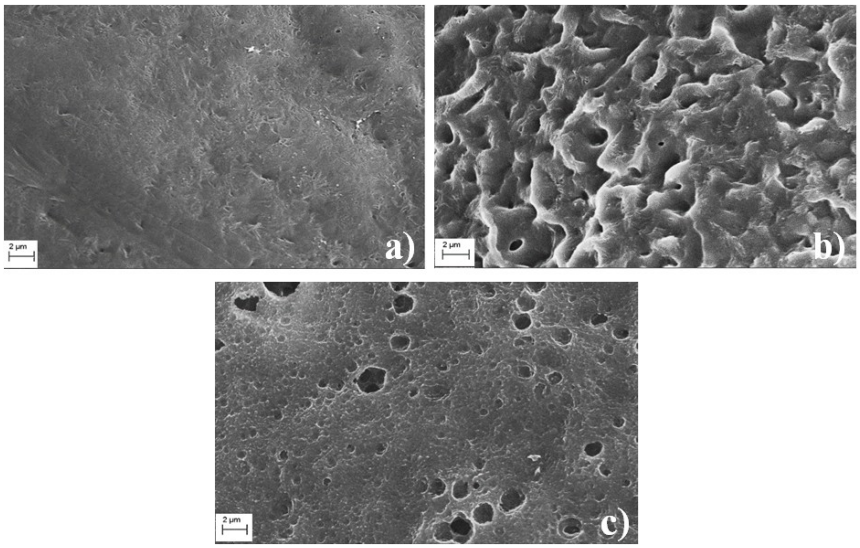

Figure.13 *a) Micrograph of the surface of the untreated scaffold; b) Micrograph of the surface of the NaOH treated scaffold; c) Micrograph of the surface of the plasma treated scaffold*

3.5. Qualitative MicroCT analisys

In order to evaluate scaffolds morphology, we performed a microCT analysis. The optimized processing conditions lead to sintered microspheres scaffolds with a well defined three-dimensional microstructure, as illustrated before, in which the microspheres are packed together with a precise geometry and connecting necks are uniformly distributed. Scaffold porosity is highly interconnected. MicroCT analysis shows no significant structural differences between NaOH or plasma treated scaffolds and those untreated. (Figure.14)

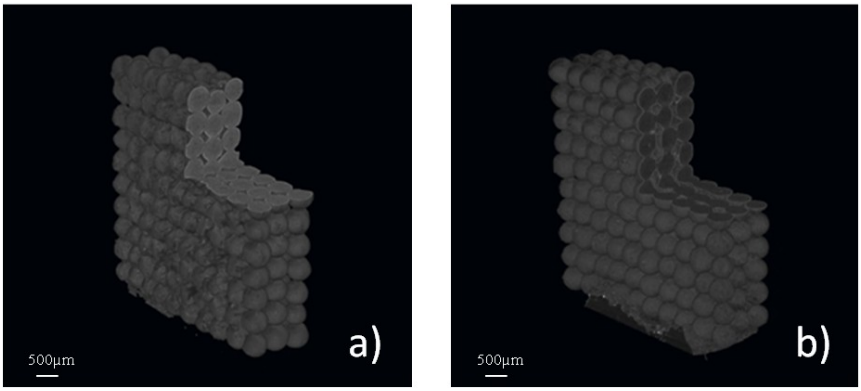

Figure.14 *Effect of different surface treatment on scaffold structure*

In accordance with the qualitative microCT analysis, it is clear that alkaline and plasma treatments did not affect the overall architecture of the scaffolds.

A mechanical characterization of the samples was performed to determine their compressive strength, elastic modulus and deformation. From the data derived from each sample compression tests, stress-strain graphs were obtained (data not shown). Compressive modulus was calculated for each sample from the slope of the linear region of the stress–strain curve. Compressive moduli of each scaffold type were calculated as the average of same type samples. The graph in Fig. 15 compares the compressive moduli of each scaffold type. Tested samples show an elastic modulus in the range of 17-28 MPa approximately. Compressive moduli of scaffolds treated with plasma and NaOH are comparable, while compared to the untreated samples, a higher elastic modulus was obtained for all kinds of treatment performed.

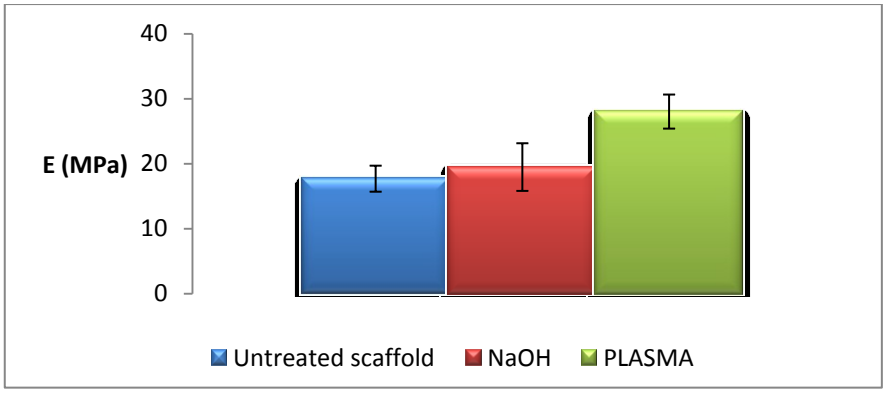

Figure.15 *Compressive modulus treated scaffold*

In both cases the order of magnitude of the elastic modulus of untreated scaffolds is consistent with that reported in literature for the ordered-porous scaffolds [93] [94].

3.6. Cells adhesion

In order to observe the effect of surface treatment on the adhesion, proliferation, and differentiation of cells, HUVECs cells were cultured on the scaffolds with different treatments. No cells morphology difference is noticeable 6 hours after seeding regardless of treatment (Figure 16). In all three micrographs the cells morphology is equal, indicating that the different treatments do not affect the morphology.

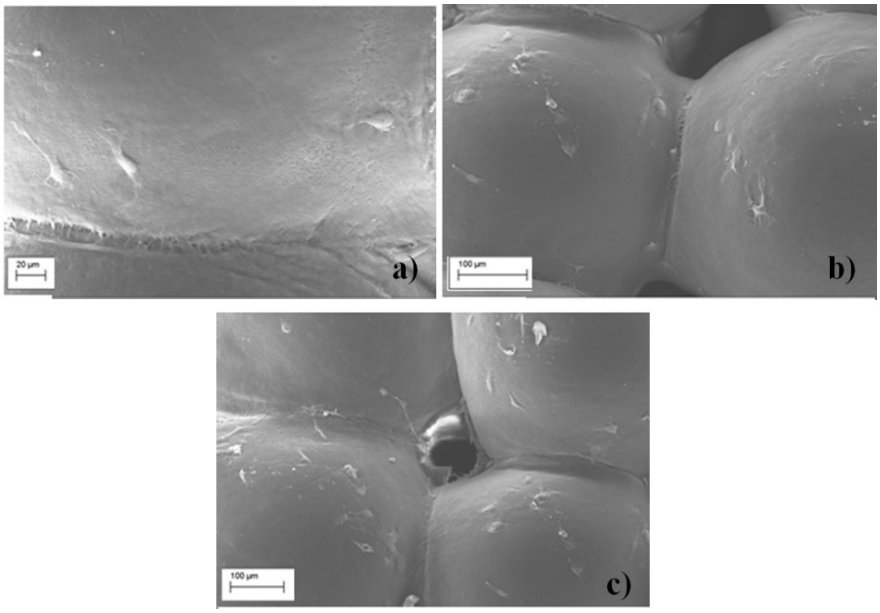

Figure.16 *Micrographs of cells on scaffolds: a) untreated, b) NaOH/EtOH treated and c) Plasma treated.*

Conversely, there is a noticeable difference in the number of cells adhering on the matrix surface. Plotting this number versus the type of surface treatment (Fig. 17), it can be observed that in both the scaffolds treated, cell adhesion is greater than the non-treated case and it is maximum for plasma in particular. This, as already pointed out, may be due to the greater number of polar components and the increased roughness in the plasma treated samples.

.

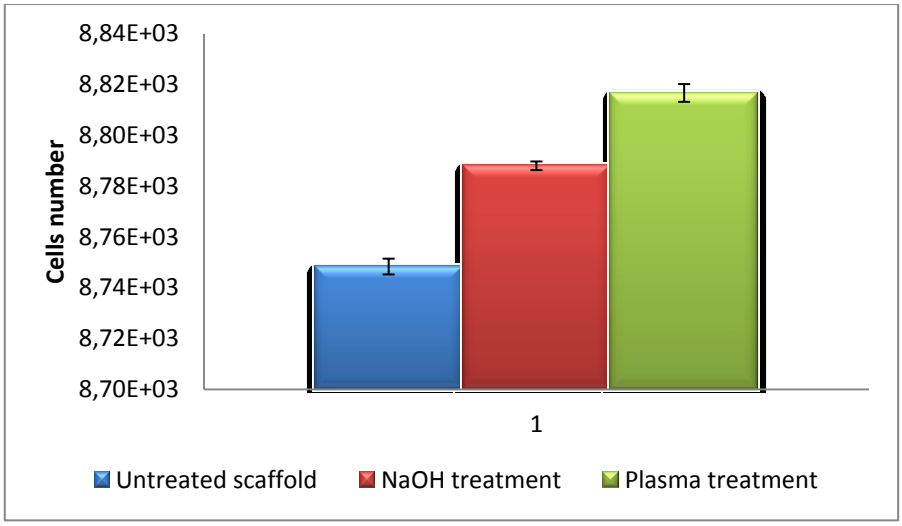

Figure.17 *type of treatment performed on the surface of the scaffold in function of cell adhesion*

3.7. QK peptide and RP characterization

Peptides were synthesized by SPPS and purified by RP-HPLC. All peptides were obtained in good yields, in high pure and homogenous forms as assessed by (Q-TOF) LC-MS. Peptide identity was verified by ESI spectrometry and a comparison of experimental and calculated MW is reported below. Table.8. HPLC and (Q-TOF) LS-MS of QK peptide and RP shown in Figure 18 and 19.

	Molecular weight Theoretical, (g/mol)	Molecular weight Experimental, (g/mol)
QK	1952,33	1952,11
RP	1661,02	1660,99

Table.8 *QK and RP peptide molecular weight*

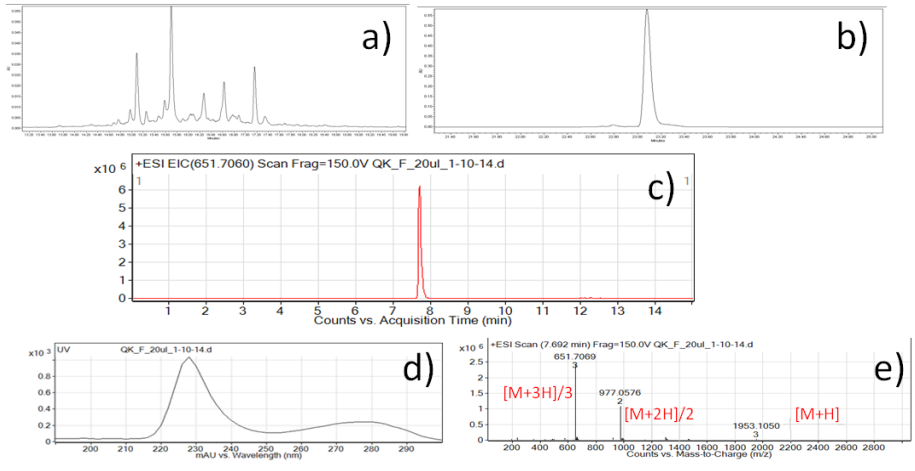

Figure.18 *LC-MS analysis of QK peptide*

RP-HPLC profile revealed at 280nm; b) UV absorption spectra of the peak; c) EIC spectra of m/z 651.7060±0.500 d) (Q-TOF) LC-MS spectrum of the peak at RT: 7.629min

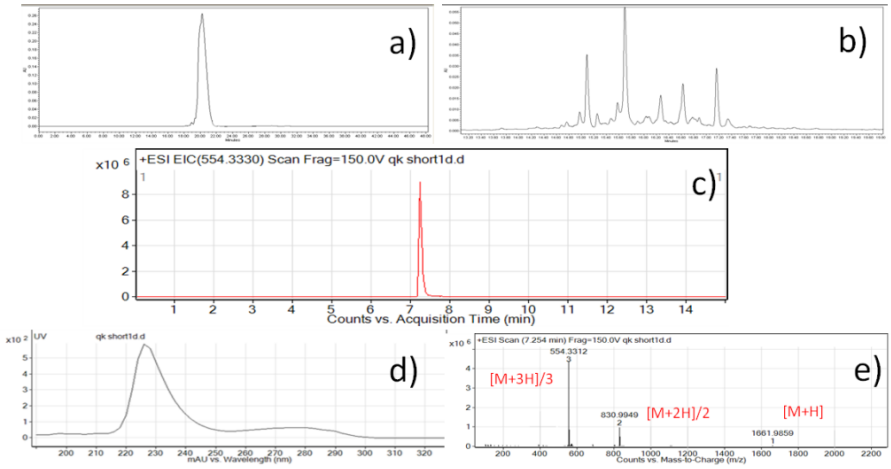

Figure.19 *LC-MS analysis of RP*

RP-HPLC profile revealed at 280nm; b) UV absorption spectra of the peak; c) EIC spectra of m/z 554.3330±0.500 d) (Q-TOF) LC-MS spectrum of the peak at RT: 7.254min.

3.8. Efficiency encapsulation and release kinetics analysis by (Q-TOF) LC-MS

To overcome problems related to QK peptide quantification in (Q-TOF) LC-MS, we resorted to the use of an internal standard. A standard curve, at known concentration, of the standard peptide, has been developed in which the area of the EIC peak has been associated uniquely with the amount of peptide. Standard peptide was added in all experiments to determine the amount of QK peptide present in the mixture degradation and release. Ionization ability of the instrument in each experiment is defined comparing the standard EIC peak area and its standard curve. Comparing the

peak area of the standard peptide with the unknown of QK, we estimated univocally the amount of peptide in each mixture.

3.9. PLGA microparticles characterization

The morphology of the two types of microspheres produced was evaluated by SEM. In order to underline the size distribution and surface appearance of the individual microspheres, we show in Figure 20 two micrographs at different magnification for each microsphere type. The microspheres look quite monodisperse and spherical in shape, regardless of formulation. The PLGA-poloxamer microspheres showed a smooth surface with micrometric pores (about 1 μm); conversely on the PLGA microspheres no pores or cavities were observed.

As the SEM micrographs of the microspheres sections show, the inner structure of the PLGA-poloxamer microparticles contains a dense pore network; however, microspheres without poloxamer had a more compact matrix-type structure (Fig. 21).

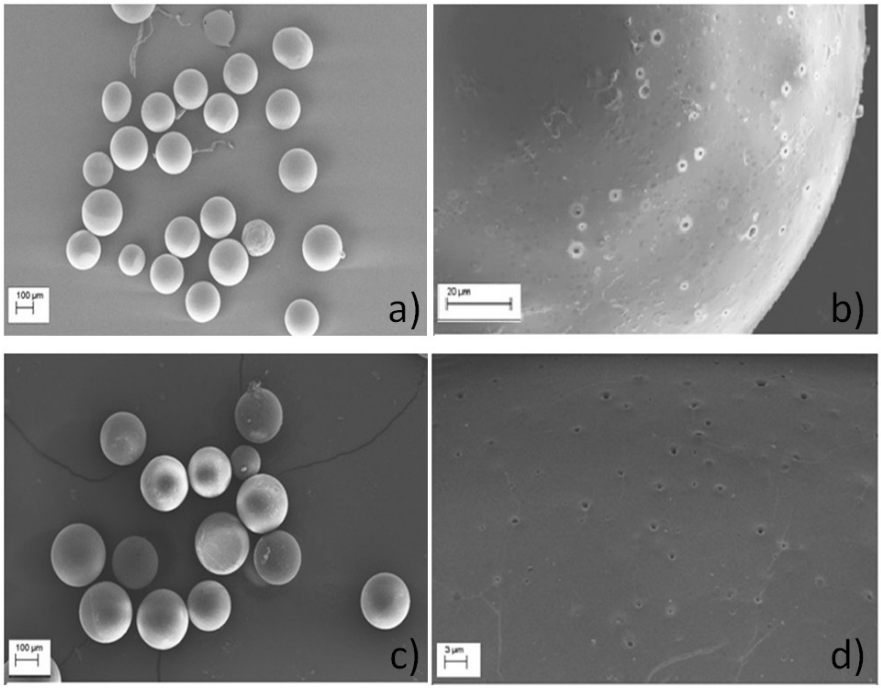

Figure.20 *micrographs of PLGA microphores at different magnification; a), b)PLGA-Poloxamer microspheres; c), d) PLGA microspheres*.

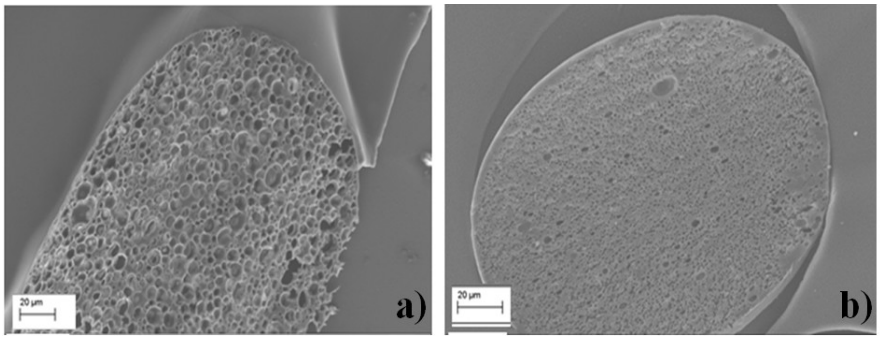

Figure.21 *a) micrographs of sections of PLGA-poloxamer microspheres; b) micrograph of section of PLGA microspheres.*

This morphological difference can affect the release of the encapsulated growth factors. A fast release of the bioactive agent is supported by the presence of a dense pore network, as in the case of

PLGA-Poloxamer microspheres, while the encapsulated protein in the case of PLGA microspheres releases in controlled and prolonged manner because of a surface without pores and a volume with few cavities,

3.10. QK encapsulation efficiency and QK in vitro release from MS

Table.9 shows the QK encapsulation efficiency of microspheres prepared by multiple emulsion/solvent evaporation (W/O/A). The specific formulation conditions gave PLGA-poloxamer microparticles with a QK encapsulation efficiency of about 73% (72.7 ± 2, 9% of QK; 1.2 ± 0, 1 µg QK for mg of microspheres). On the other hand PLGA-only microparticles have an encapsulation efficiency of 46% (45 ± 4, 6% of QK; 0.7 ± 0, 1 µg QK for mg of microspheres).

Formulation	Encapsulation efficiency	µg QK/ mg microspheres
PLGA-Poloxamer	72.7 % ± 2,9	1.2 ± 0,1
PLGA	45% ± 4,6	0.7 ± 0,1

Table9 *PLGA-poloxamer and PLGA microparticles encapsulation efficiency and µg QK/mg microspheres*

The high encapsulation efficiency of PLGA-Poloxamer microparticles could be related to a possible tendency of the peptide to interact with the poloxamer during the w/o primary emulsion. In vitro release tests were performed in order to analyze the effect of the two microparticle formulations. The QK release profile by PLGA microparticles is shown in Figure 22, and is expressed as µg of QK released in active form for 1 mg of microspheres as a function of time. As can be seen from the graph, the microparticles show an initial burst release of QK, in the first day of incubation, (32.7 ± 4.2% of QK), followed by a stable release.

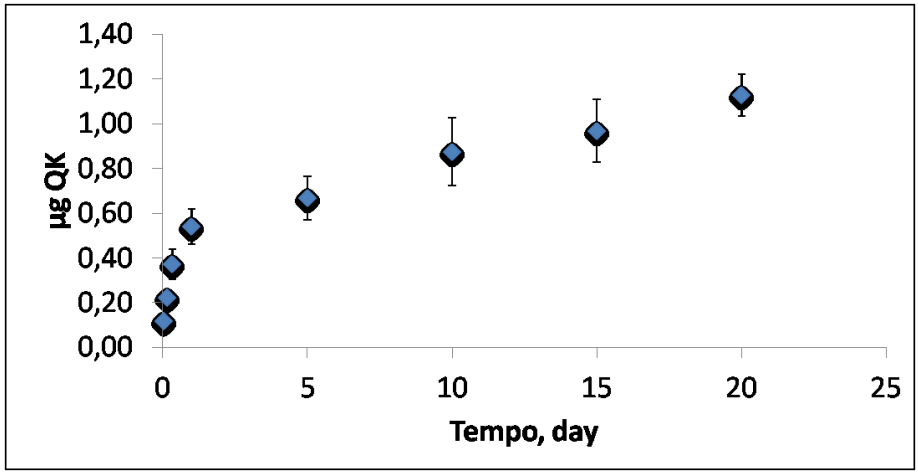

Figure.22 *Release profile of QK by PLGA microparticles (µg\mg MS)*

These results suggest that the microparticles manufactured, when placed in three-dimensional substrates, have an excellent potential of promoting the activation of angiogenic processes, if careful control of the GF dose is provided.

Conversely, PLGA-Poloxamer showed a higher release of peptide during the bust phase (89, 9 ± 3, 3% of QK) after just one day of

incubation. The higher QK release from the formulation containing poloxamer could be related to the stabilizing effect of the w/o primary emulsion. In particular the presence of poloxamer hinders the formation of the stabilizing film formed by the interaction between the peptide and the polymer which stabilizes the microdroplets of the w/o primary emulsion. This phenomenon leads to the coalescence of the aqueous microdroplets and, thus, to a more porous structure which goes from the inside to the surface of particles.

3.11. QK in vitro release from scaffold

The release profile of QK by the bioactive scaffolds prepared is expressed as μg of QK/scaffold released in active form as a function of time. We observe an initial release of QK in the first day of incubation, followed by a controlled release of QK. The Figure.23 compares the release kinetics of QK from PLGA-Poloxamer and PLGA microspheres in a scaffold, expressed as μg QK per mg of microspheres

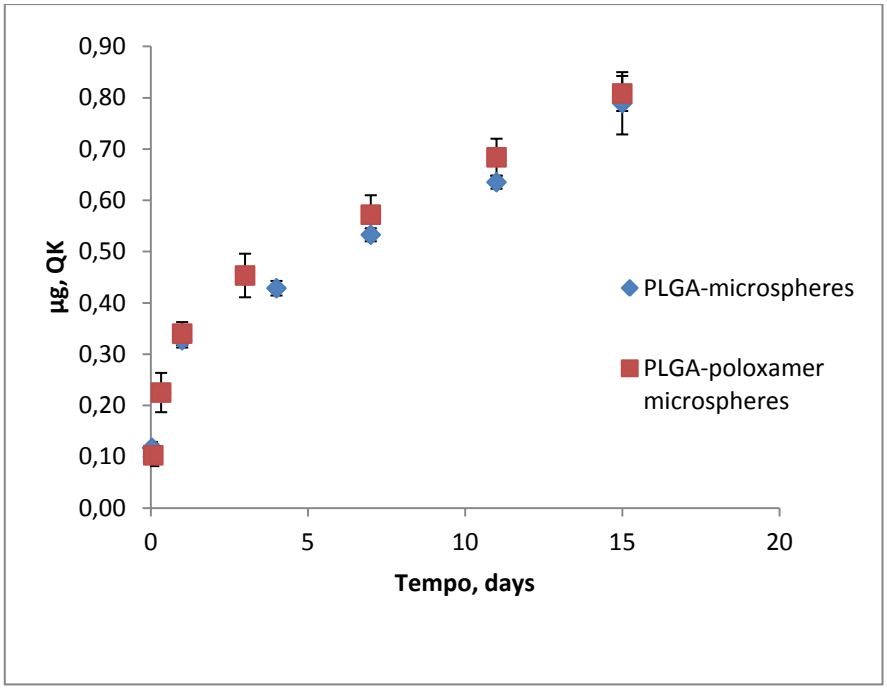

Figure.23 *Release profile of QK by bioactive scaffold (µg\scaffold)*

This comparison shows that the trend of the release kinetics is practically the same, but much slower compared to the "free" microparticles (Fig. 24). This phenomenon can be ascribed to the process of sintering that through the formation of the junction points between microspheres reduces the surface area available to the free factor. In addition, it is possible that the peptide on the surface of the microspheres is removed during the sintering step in which there are several washings with ethanol.

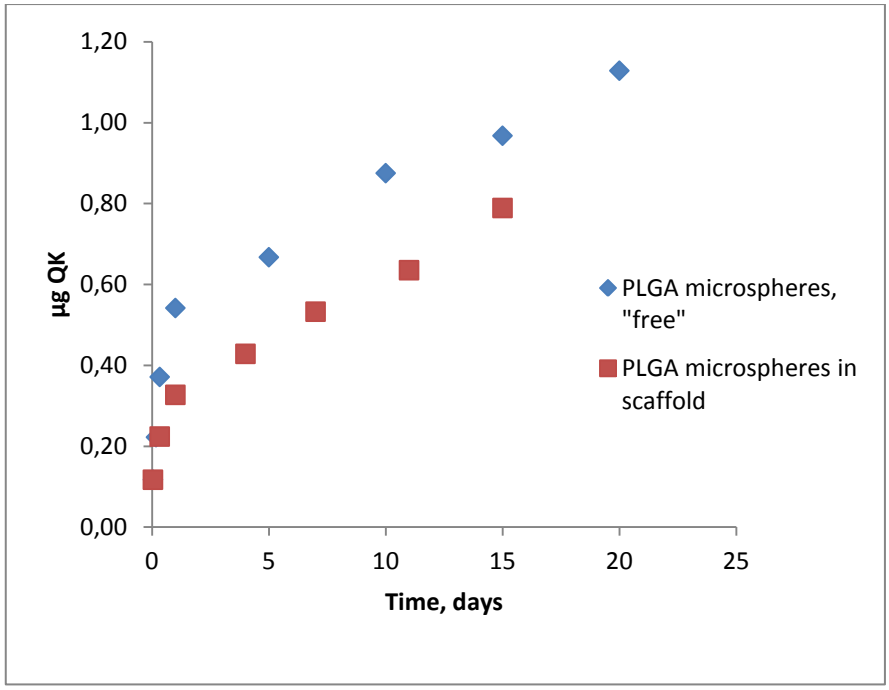

Figure.24 *Comparison between the release kinetics of QK from scaffolds and single microparticles (µg QK / mg MS)*

These results suggest that the bioactive scaffolds made from microparticles containing QK, have an enormous potential in inducing the formation of new blood vessels and consequently to promote the formation of a highly vascularized tissue.

3.12. Bioactivity Assay

The angiogenic potential of the encapsulated peptide was tested by spheroids angiogenesis assay on the basis of the angiogenic response measured in terms of sprouts number. We assayed the

effect of the peptide released by PLGA microparticles with and without poloxamer suspended in PBS or embedded in collagen. As shown in Figure 25, nude PLGA microparticles maintained an intact angiogenic potential of the encapsulated peptide compared to PLGA-poloxamer depots (QK 40ng/ml)

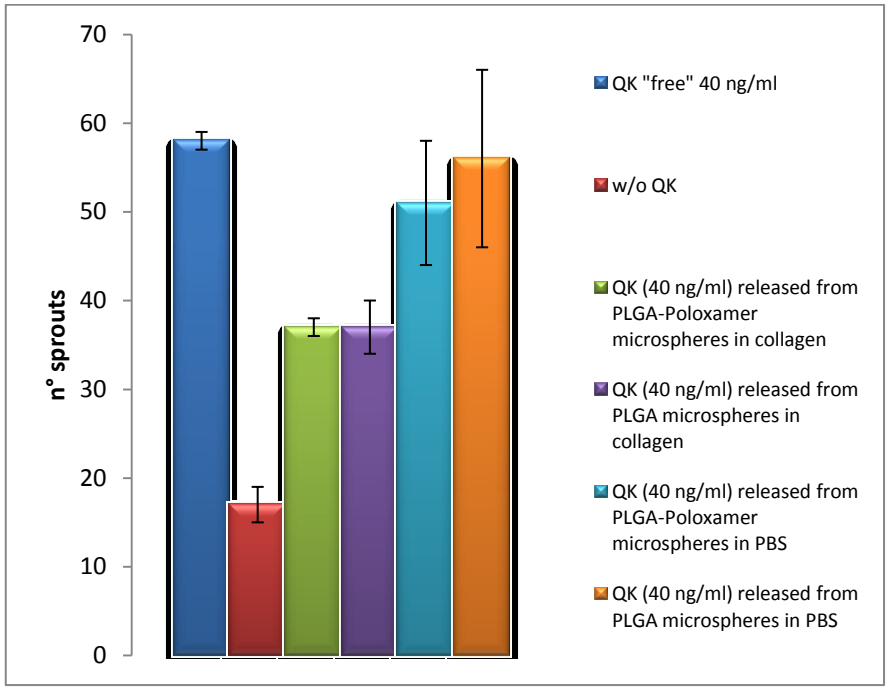

Figure25 *Difference in number of sprouts generated by QK released by microspheres in PBS and in collagen matrix*

Figure 26 shows confocal images of released QK bioactivity from two different formulations of microspheres in PBS on HUVEC spheroids embedded in the collagen matrix. More groups were tested in order to evaluate the dose-response correlation of the peptide released by microparticles embedded in collagen together with the spheroids.

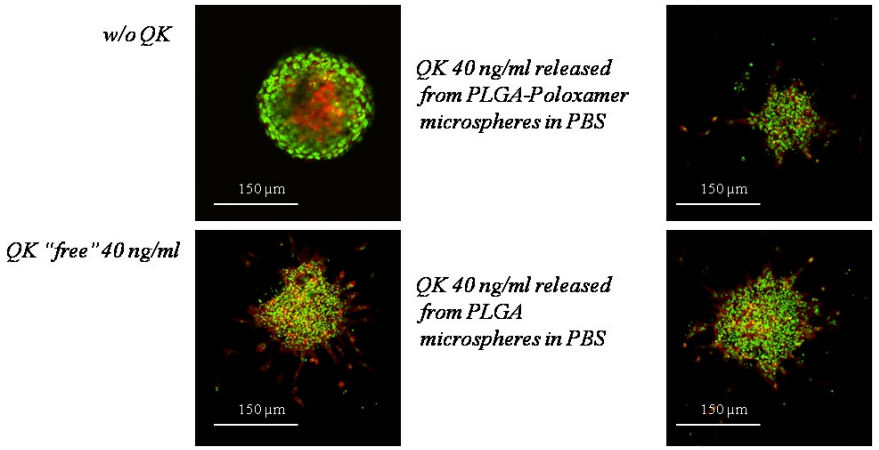

Figure.26 *Sprouting of HUVEC spheroids embedded in collagen*

We assayed the effect of three different concentrations of QK, 40, 80 and 160 ng/ml, in comparison to 40 ng/ml of free peptide. In Figure 27 there is a clear correspondence between QK concentrations and the degree of angiogenic response, confirming the reliability of our release system. Figure 28 shows confocal images of HUVEC spheroids embedded in the collagen matrix at different QK concentrations. As shown, there is a clear increase of sprouts number, in response to high concentrations of peptide. (Nuclei are in green and actin filaments are in red)

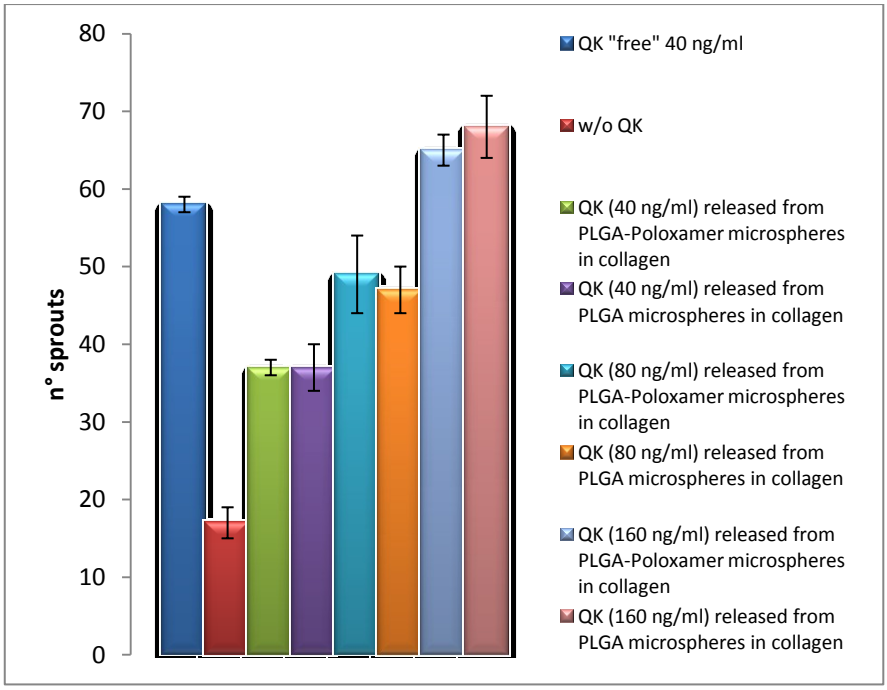

Figure .27 *Dose-response correlation of QK released by microparticles embedded in collagen on number of sprouts.*

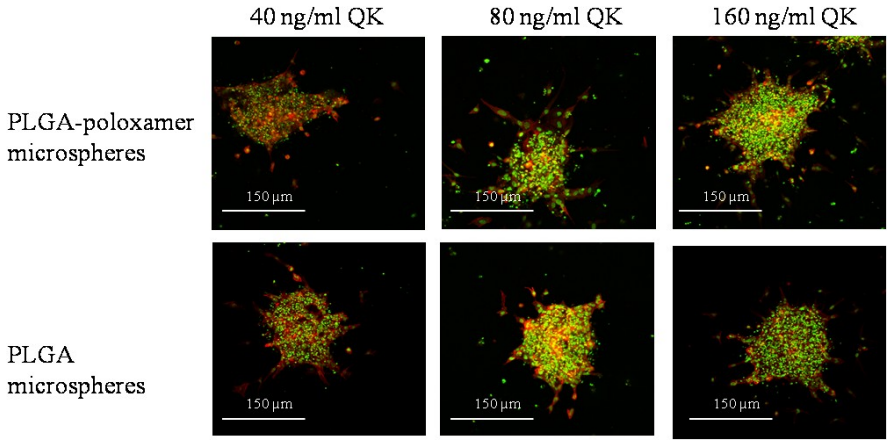

Figure.28 *Sprouting of HUVEC spheroids embedded in collagen with different QK concentration*

References

1. Luciani, A., et al., *Solvent and melting induced microspheres sintering techniques: a comparative study of morphology and mechanical properties.* Journal of Materials Science: Materials in Medicine, 2011. **22**(9): p. 2019-2028.
2. Eshraghi, S. and S. Das, *Mechanical and microstructural properties of polycaprolactone scaffolds with one-dimensional, two-dimensional, and three-dimensional orthogonally oriented porous architectures produced by selective laser sintering.* Acta Biomater, 2010. **6**(7): p. 2467-76.
3. Ouyang, J., et al., *Biomechanical characteristics of human trabecular bone.* Clinical Biomechanics, 1997. **12**(7-8): p. 522-524.
4. Porter, B.D., et al., *Mechanical properties of a biodegradable bone regeneration scaffold.* J Biomech Eng, 2000. **122**(3): p. 286-8.

Chapter 4

4. Conclusion

This research work was focused on the fabrication and analysis of three-dimensional PCL scaffolds containing bioactive micro depots releasing pro-angiogenic peptides *in-vitro*.

The first step aimed towards the optimization of a bottom-up fabrication technique in which single PCL microparticles are sintered chemically by a mixture of solvent/ non-solvent (Anisole/ ethanol). The effects of Anisole concentration on the scaffold structure, such as total percentage of pores, interconnection of pores network and mechanical properties, were thoroughly evaluated. In order to identify the optimal conditions for the fabrication of such structures, mechanical compressive stress tests, and morphological analyses by computed microtomography were performed. The results presented show that increasing anisole concentration decreases the percent porosity of the scaffold, which has been correlated to the swelling phenomenon of PCL microspheres. At the same time anisole concentration also influences the mechanical properties. A modification of solvent concentration had a significant effect on the elasticity of the polymeric structure. A higher solvent concentration gives rise to a greater elastic modulus.

To improve cells adhesion and proliferation 2 types of treatments were performed on the surface of PCL scaffold: Plasma and basic hidrolys by NaOH/Ethanol solution. It was demonstrated that both treatments increase the number of adherent cells, without any significant alteration of the scaffolds structure. Plasma treatment, in particular, leads to an increase in elastic moduli and to a high number of cells interacting with the surface of the scaffold.

The second phase concerned the process optimization of PLGA microspheres synthesis. These DDS were later used as depots of QK, an angiogenic peptide mimicking Vascular Endothelial Growth Factor. To study the peptide bioactivity *in-vitro* HUVEC spheroids assays were performed. In particular, we have shown that the biological activity of QK, at 24 hours, is not altered by the formulation type of PLGA microspheres (with or without poloxamer). We also confirmed the reliability of our delivery system and assayed the effect of three different concentrations of QK on HUVEC spheroids in order to evaluate correspondence between QK concentrations and the degree of angiogenic response. In vitro studies of the release kinetics and bioactivity assays demonstrated that the PCL scaffold bioactivated with PLGA microparticles could be a potential tool for inducing the formation of the new blood vessels *in-vivo*.

In conclusion, the bottom up approach allows the fabrication of an ordered highly standardized structure, with predictable mechanical and morphological properties and capable of releasing - from embedded, suitably designed micro depots - active biological factors in a predetermined crono-programmed manner.